Hindawi Publishing Corporation
Advances in Meteorology
Volume 2015, Article ID 352380, 21 pages
http://dx.doi.org/10.1155/2015/352380

Research Article

The Variability of Arctic Sea Ice Extent from Spring to Summer and Its Linkage to the Decline of SIE in September

Zhenhao Bao,[1] Gordon Huang,[1] Jinliang Liu,[2] and Hengchun Ye[3]

[1]*Institute for Energy, Institute for Energy, Environment and Sustainable Communalities, University of Regina, Regina, SK, Canada S4S 0A2*
[2]*Department of Earth and Space Science and Engineering, York University, Toronto, ON, Canada M3J 1P3*
[3]*Department of Geosciences and Environment, California State University, Los Angeles, CA 90032, USA*

Correspondence should be addressed to Zhenhao Bao; zhenhao_bao@yahoo.com

Received 2 January 2015; Revised 14 May 2015; Accepted 14 May 2015

Academic Editor: Hiroyuki Hashiguchi

The satellite record analysis for monthly differences of Arctic sea ice extent (SIE) shows that the most significant accelerated monthly sea ice reduction occurred between June and July although, on average, the largest sea ice reduction occurred between July and August. The monthly difference of June minus July (JJ) SIE has the strongest correlation with September SIE, with a correlation coefficient of −0.786 (original time series) and −0.625 (detrended time series) at confidence level of 99%. Furthermore, it is found that the correlation coefficient between JJ SIE and July minus August (JA) SIE is so low (0.068) that they can be thought to be independent from each other, considering that the JA SIE is also significantly negatively correlated to September SIE. A simple regression forecasting model for September SIE was established using monthly SIE differences for the JJ and JA. This study also shows that the JJ SIE is significantly correlated not only with sea level pressure (SLP) in polar regions and midlatitudes over eastern Atlantic in July, a pattern which resembles the negative phase of North Atlantic Oscillation (NAO), but also with sea surface temperature (SST) in midlatitudes over central North Pacific in the preceding spring.

1. Introduction

The decline of Arctic sea ice has been one of the most striking changes to associate with global-scale air temperature change, particularly to global warming [1]. In recently global warming history, there are two key periods in decadal scales, one 1930–50's and the other from the end of 1970's until now [2]. The rapid climate change in high-latitude regions over Northern Hemisphere is mainly characterized by rapidly diminishing sea ice and snow cover variability (e.g., [3–16]). During the last decades, the Arctic sea ice has significantly decreased (e.g., [17–19]). Moreover, this phenomenon seems to continue and several current climate models have predicted that the now clearly accelerating decline of summer ice in recent decades will be a goner far sooner than the end of the century [20–22].

The potential dynamical causes of observed decrease in Arctic sea ice in September have been discussed in many scientific literatures (e.g., [23–29]). Particularly, in the summers of 2007 and 2012, Northern Hemisphere sea ice reached new record lows on the Arctic Ocean. Sea ice extent as a sensitive physical variable in climate systems is mainly linked to air-sea-ice interaction processes among the oceans, atmosphere, and cryosphere, and its variability directly influences global surface air temperature and sea surface level change. The reduced sea ice in sunny summer has a direct impact on the Arctic surface's physical processes by reducing albedo and absorbing more solar radiation and results in a faster surface air temperature increase. During spring and summer, the presence of open water in Arctic always allows more solar direct radiation energy to be absorbed while a stable atmospheric circulation situation exists in polar region, prolonging the melt season until the end of September [30].

Recent reduction trends about sea ice cover have been explained by changes in atmosphere circulation associated with the increasing cyclone frequencies [11, 23, 31, 32]. Large-scale surface (925 hPa) wind in summer (the average for June through September) and winter (the average for January

through May) plays an important role in linking to Arctic sea ice in September [33].

Ogi and Yamazaki [34] analysed the Arctic sea ice and its associated summer northern annular mode, and though the difference in sea ice extent (SIE) between May and September has a significant correlation with the summer Northern Hemisphere Annular Mode. Zhang et al. [29] pointed out that the record low ice cover and the unusually warm ocean surface waters in summer 2007 lead to a substantial reduction in ice thickness in 2008 based on an ice-ocean model.

The monthly SIE Index provides a quick look at Arctic-wide changes in sea ice, and its variability from higher in March to the lower records in September experiences a slower sea ice absorbing heat and melting processes. Predicting seasonal to interannual variability of the sea ice cover has received much attention by climate scientists [35, 36]. Drobot et al. [35] discuss the development of a simple statistical model for forecasting the annual Pan-Arctic minimum sea ice extent based on mean monthly weighted indices of sea ice concentration, surface skin temperature, surface albedo, and downwelling long-wave flux at the surface. There are better forecast skills for predictions of the observed September SIE for the Pan-Arctic region with a 0.77 correlation coefficient for six-month lead (from March) [36]. September SIE is significantly correlated to the SIE in the previous August and July, and thus these months show a predictive skill of the summer minimum SIE [37].

The Arctic sea ice loss in September has important consequences in Arctic community and regional environment considering the increasing ship traffics and safety. Although there are many physical factors associated with the likelihood of an ice-free Arctic in summer, their physical processes remain unclear. In order to better understand and predict the Arctic SIE in September, it is necessary to further examine monthly-to-monthly SIE differences during warm season connecting to this complex phenomenon.

This study will focus on investigating the monthly differences of SIE from April to September and their monthly-to-monthly variability in relation to the decline of the September SIE. Furthermore, we will examine which monthly SIE differences have more important contributions and significant impact on the September SIE decrease and analyze their associations with atmosphere-ocean circulation pattern anomalies. Finally we will compile a set of prognostic variables to establish a simple forecasting relationship for the September SIE. This paper is structured as follows: data and methodology are described in Section 2, and analysis of monthly SIE differences and large-scale atmosphere-ocean circulation indices and patterns are presented in Section 3, with summary and conclusions in Section 4.

2. Data and Methodology

The monthly sea ice extent (SIE) dataset from April to September for 1979–2012 is from the satellite-derived observation records available from the National Snow & Ice Data Center (NSIDC) (http://nsidc.org/data/docs/noaa/g02135_seaice_index/). In addition, the North Atlantic Oscillation (NAO) index (http://www.esrl.noaa.gov/psd/data/correlation/nao.data) which represents a climatic phenomenon in the North Atlantic Ocean about fluctuations due to the difference of sea level pressure between the Icelandic Low and the Azores High [38] and the Arctic Oscillation (AO) index which is a global-scale climate mode characterized by winds circulating counterclockwise around the Arctic at around 55°N latitude (http://www.cpc.ncep.noaa.gov/products/precip/CWlink/daily_ao_index/monthly.ao.index.b50.current.ascii) [6, 39] are acquired form the National Center for Environmental Prediction (NCEP)/National Center for Atmospheric Research (NCAR) reanalysis dataset [40]. The atmosphere-ocean gridded datasets such as monthly sea level pressure (SLP), 700 hPa and 500 hPa geopotential heights (GHT) with a horizontal resolution of 2.5° latitude and longitude over north of 30°N, and sea surface temperature (SST) with a horizontal resolution of 2.0° latitude and longitude over north of 10°N are also used from the NCEP/NCAR reanalysis for the same period.

In order to investigate the climate characteristics of monthly SIE differences in the Arctic, the five monthly SIE differences from April to September, April minus May (AM), May minus June (MJ), June minus July (JJ), July minus August (JA), and August minus September (AS), are first calculated based on the SIE dataset from 1979 to 2012.

These monthly SIE differences from April to September reflect the sea ice melt and gradually decreasing processes in the warm season, and they are responsible for a greater energy and mass exchanges among sea ice, water, and air associated with atmosphere-ocean circulation anomalies in middle and high latitudes.

The Arctic Oscillation (AO) and Northern Atlantic Oscillation (NAO) are two important indices in relation to climate change and large-scale circulation anomalies (e.g., [5, 36, 38, 41, 42]). In this study, we will examine whether the NAO and AO index anomalies have some impacts upon monthly SIE differences.

The multiple linear regression [43] is used to model and analyze the relationship between two or more explanatory variables and a response variable with an important goal of making useful predictions of the response variable in this study, which is an extension of simple linear regression analysis and can be used to assess the association of September SIE with the monthly SIE differences from April to August. Using the established regression equation, we are able to reconstruct, analyze, and compare the sea ice extent time series with the satellite records of SIE in September.

3. Results

3.1. The Relationship between Monthly SIE Differences in Warm Season and the SIE in September. Figure 1 shows the time series of the SIE differences for AM, MJ, JJ, JA, and AS from 1979 to 2012, in which there are apparent increasing trends for all but AM indicating accelerated monthly declining speed of sea ice starting May to September. Table 1 lists the corresponding standard variance, mean and linear trend rate for the five time series of monthly SIE differences, and

Table 1: Statistical analyses of the five sea ice extent (SIE) differences (unit: millions of square kilometers (Mkm^2)) for April minus May (AM), May minus June (MJ), June minus July (JJ), July minus August (JA), and August minus September (AS) during 1979–2012 and the correlation between September SIE and these five SIE differences. Trends significant at 95% and 99% confidence level are indicated with asterisks as (∗5) and (∗1); correlation coefficients higher than 0.339 and 0.435 are defined as at 95% (∗5) and 99% (∗1) confidence levels, respectively.

Statistics value\SIE difference	Apr-May	May-Jun	Jun-Jul	Jul-Aug	Aug-Sept
Mean (Mkm^2)	1.37	1.53	2.24	2.48	0.72
Standard variance (Mkm^2)	0.19	0.34	0.41	0.29	0.27
Liner trend rate (per year)	−0.0047	0.0139^{*5}	0.0263^{*1}	0.0062	0.0135^{*1}
Maximum (Mkm^2)/year	1.76/1983	2.28/2010	3.37/2007	3.22/2012	1.32/2008
Minimum (Mkm^2)/year	0.98/2007	0.66/1989	1.45/1983	1.75/2001	0.19/1980
The corr. of SIE in Sept	0.163	-0.499^{*1}	-0.786^{*1}	-0.477^{*1}	-0.691^{*1}
The corr. after detrending	−0.092	−0.323	-0.625^{*1}	-0.517^{*1}	-0.598^{*1}

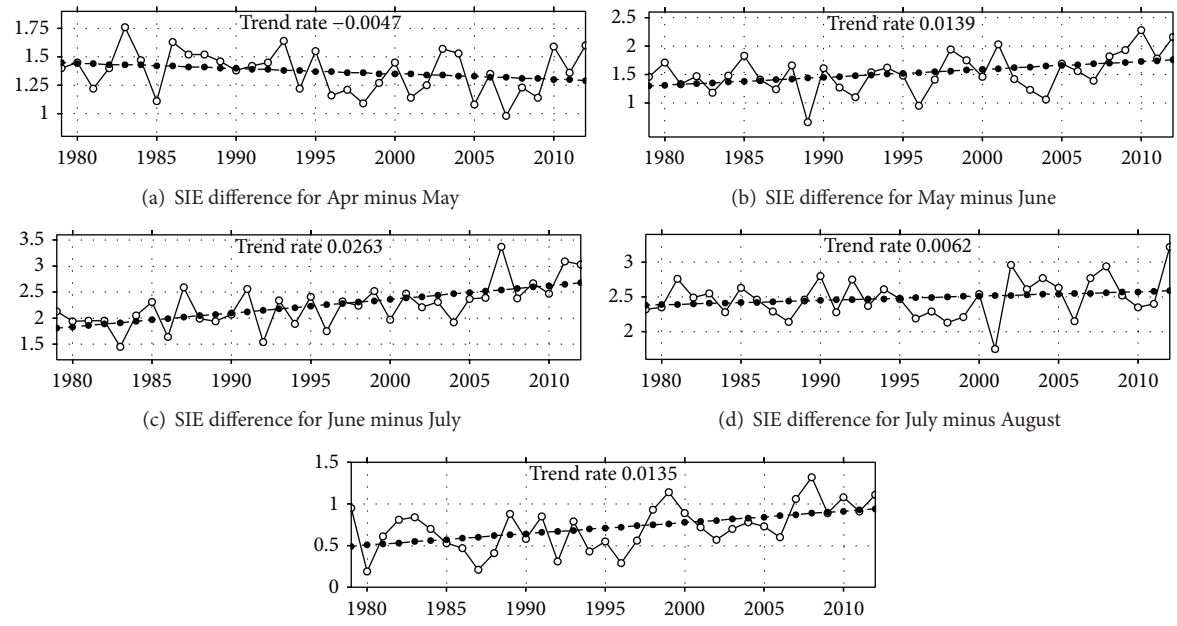

(a) SIE difference for Apr minus May

(b) SIE difference for May minus June

(c) SIE difference for June minus July

(d) SIE difference for July minus August

(e) SIE difference for Aug minus Sept

Figure 1: The time series of sea ice extent (SIE) differences and their linear curves (unit is millions of square kilometers) for 1979–2012: (a) for April minus May (AM), (b) for May minus June (MJ), (c) for June minus July (JJ), (d) for July minus August (JA), and (e) for August minus September (AS).

their correlation with the SIE in September for the same time period. The mean of JA SIE difference, 2.48 millions of square kilometers (Mkm^2), is the highest among the five time series, whereas the mean for AS is the lowest, 0.72 Mkm^2, less than one-third of the mean in JA. The maximum JA SIE value of 3.22 Mkm^2 occurred in 2012, and its minimum value of 1.75 Mkm^2 appeared in 2001. The mean of the JJ SIE difference is 2.24 Mkm^2 which is the 2nd highest among the five. It is also noted that the JJ SIE difference has obviously increased since 2007 as shown in Figure 1(c). The standard variance of JJ SIE is 0.41 which is the largest in the five time series (Table 1). The linear growth rate per year is 0.0263 in JJ; SIE is much higher than 0.0062 in the JA suggesting that the highest accelerated monthly sea ice reduction occurred between June and July during time period of 1979–2012.

The correlation between the two time series of JJ and JA shows a very low correlation coefficient (0.068) which is not statistically significant and the two variables can be thought to be independent of each other. We have also examined the relationship between JA and AS and noted that their correlation coefficient is 0.204, much lower than the confidence level of 95%.

Despite the low correlation between the JJ and JA, higher negative correlations exist between each and the September SIE: −0.786 and −0.447 in JJ and JA, respectively, both at 99% confidence levels (higher than 0.435). Furthermore, after detrending the time series of monthly differences of SIE and the September SIE, it is found that both of the JJ and JA still have a significant negative correlation with the SIE in September with correlation coefficients −0.625 and −0.517

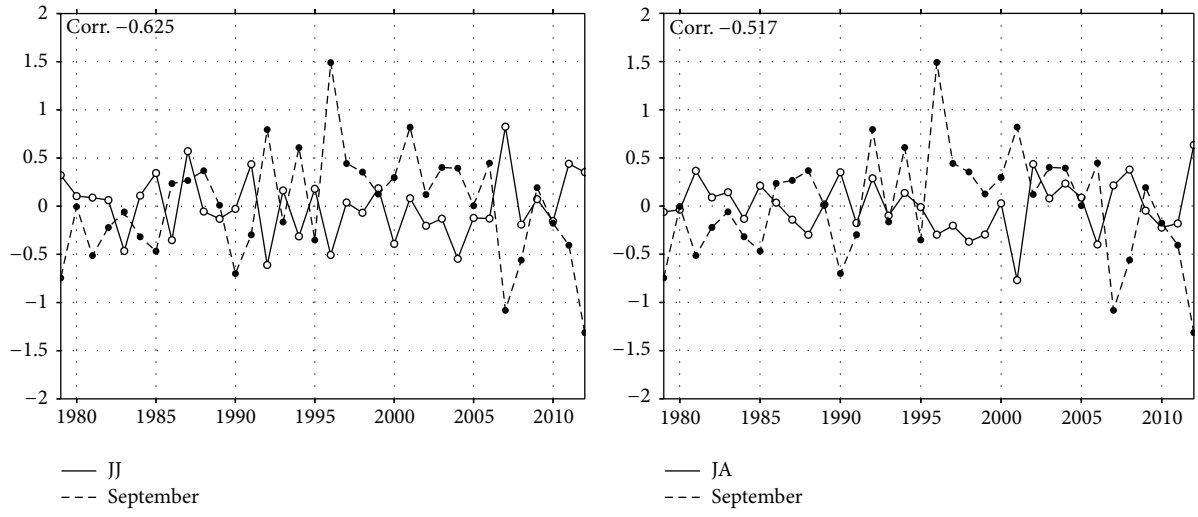

(a) JJ and Sept SIE after detrending

(b) JA and Sept SIE after detrending

Figure 2: The time series of sea ice extent (SIE) difference for JJ and JA SIE and the September SIE in 1979–2012 after detrending: (a) JJ SIE and SIE in September and (b) JA SIE and SIE in September.

(shown in Table 1). In other words, the loss of sea ice in the Arctic, with particular attention focused on the September SIE, is closely associated with monthly differences in sea ice melting processes in the two or three previous months, JJ and JA. Therefore SIE differences in JJ and JA can be used as two prognostic variables to forecast the September SIE with one to two-month lead in time.

Before 2000, the JA SIE values have been higher than those for JJ SIE except in 1987, 1991, and 1997, but after then the JJ SIE became higher and its value is over 2.0 Mkm^2 except for 2004 (1.92 Mkm^2). Meanwhile, it is noted that the JJ SIE values have significantly increased in recent years such as 2007, 2011, and 2012. The two recent recorded minimum September SIE values occurred in 2007 and 2012, which shows that the JJ SIE (3.37 Mkm^2) in 2007 and JA SIE (3.22 Mkm^2) in 2012 have the largest contributions to the decline of SIE in September, respectively. Figure 2 shows the time series of the JJ and JA SIE and the September SIE after detrending. It is noted that there are larger positive phases for JJ in 2007, 2011, and 2012 and for JA in 2007, 2008, and 2012 after 2006. In fact, the superposition of two positive phases for the JJ and JA in 2007 and 2012 results in the lowest recorded September SIE in the Arctic.

3.2. The Connections of Monthly SIE Differences to the Atmosphere Circulation Patterns. Figure 3 shows average sea level pressure (SLP) in summer (June, July, and August) from 1979 to 2012 for the north of 30°N and its correlation with the three monthly SIE differences in MJ, JJ, and JA. Examining the monthly SLP patterns during summer, it is noted that the two high pressures (North Pacific and Azores High) in midlatitudes in July are stronger than those in June and August (Figures 3(a), 3(c) and 3(e)), and there are low pressures in the Arctic during summer. In these simultaneous correlation patterns of the monthly SIE differences with SLP, the JJ and JA SIE exhibit apparent positive correlation in the Arctic and high latitudes over the Atlantic sector at above 95% confidence level (higher than 0.339); and their correlation areas are primarily located in polar regions 0–45°W (for JJ) over eastern Atlantic and 45–90°W (for JA) over western Atlantic (Figures 3(d) and 3(f)), respectively. Particularly, the correlation fields of the JJ SIE with SLP cover more pronounced and wider areas (correlation coefficient >0.5 at above 99% confidence level) while compared with the other two cases the MJ and JA. It indicates that the positive anomalies of SLP in polar regions and high latitudes over Atlantic are associated with more sea ice melt in July which is due to sunny weather and strong solar radiation absorbed by the water. In addition to the most significant positive correlation patterns occurring in high latitudes over the Atlantic sector for the JJ, the SLP in midhigh latitudes in June and July also exhibits stronger negative correlations with the MJ and JJ, separately. For example, the significant negative correlation pattern of SLP with the MJ is mainly located in Eurasian continent and North Pacific (Figure 3(b)), and the negative correlation areas partly correspond to the low SLP systems in June which is the degraded Low over Eurasian continent (Figure 3(a)). The apparent negative correlation areas of SLP with the JJ are located in midhigh latitudes over eastern Atlantic and western Europe (Figure 3(d)). From the different patterns of the three SIE differences connecting to SLP in summer, it reveals that the SLP anomalies over polar regions in July have an apparent effect on the JJ SIE variability. Furthermore, we also examined the 700 hPa and 500 hPa GHT fields connecting to the monthly SIE differences for MJ, JJ, and JA in order to compare their association with the simultaneous SLP field. The results show that the positive correlation patterns of the JJ with the 700 hPa and 500 hPa GHT in polar region become more significant than those at SLP field (Figures 3(d), 4(d), and 5(d)). But for JA, it is noted that its correlation patterns with SLP display more significant features than those at 500 hPa and 700 hPa GHT. The result

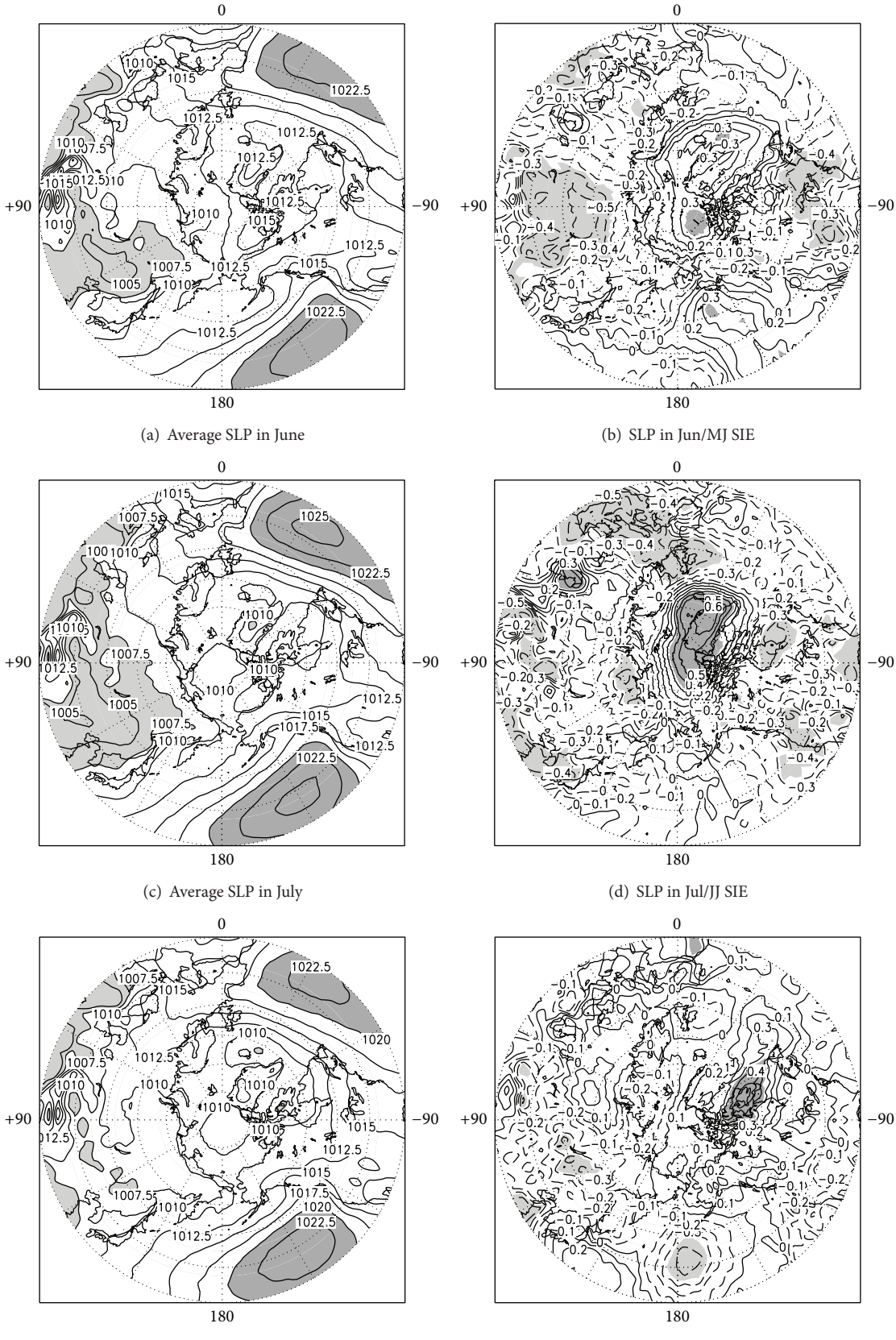

(a) Average SLP in June

(b) SLP in Jun/MJ SIE

(c) Average SLP in July

(d) SLP in Jul/JJ SIE

(e) Average SLP in Aug

(f) SLP in Aug/JA SIE

Figure 3: The monthly average sea level pressure (SLP) in June, July, and August for 1979–2012 and the correlation distribution between simultaneous monthly SLP and the monthly SIE differences over the north of 30°N: (a) average June SLP, (b) corr. between June SLP and MJ SIE, (c) average July SLP, (d) corr. between July SLP and JJ SIE, (e) average August SLP, and (f) corr. between August SLP and JA SIE.

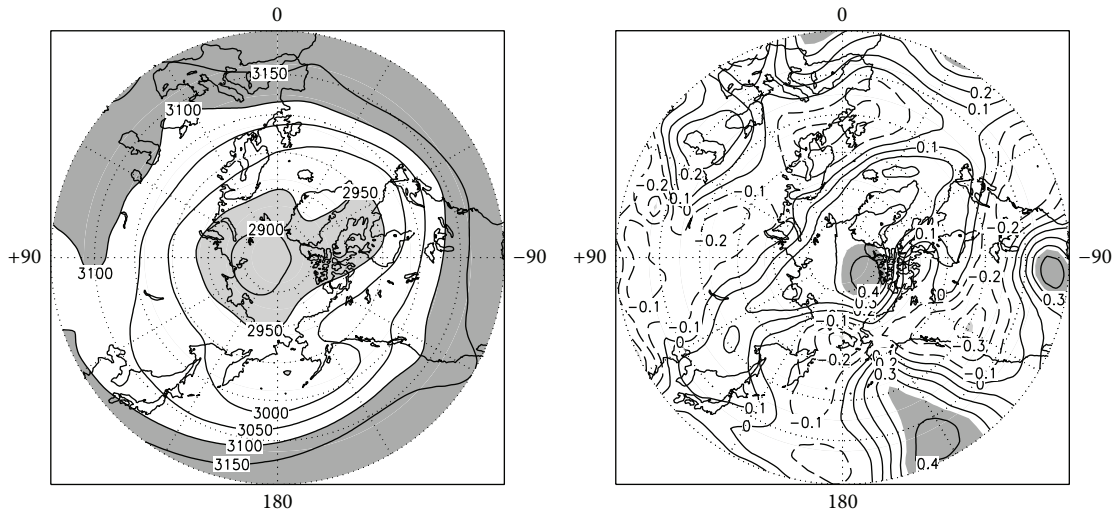

(a) Average H700 in June

(b) H700 in Jun/MJ SIE

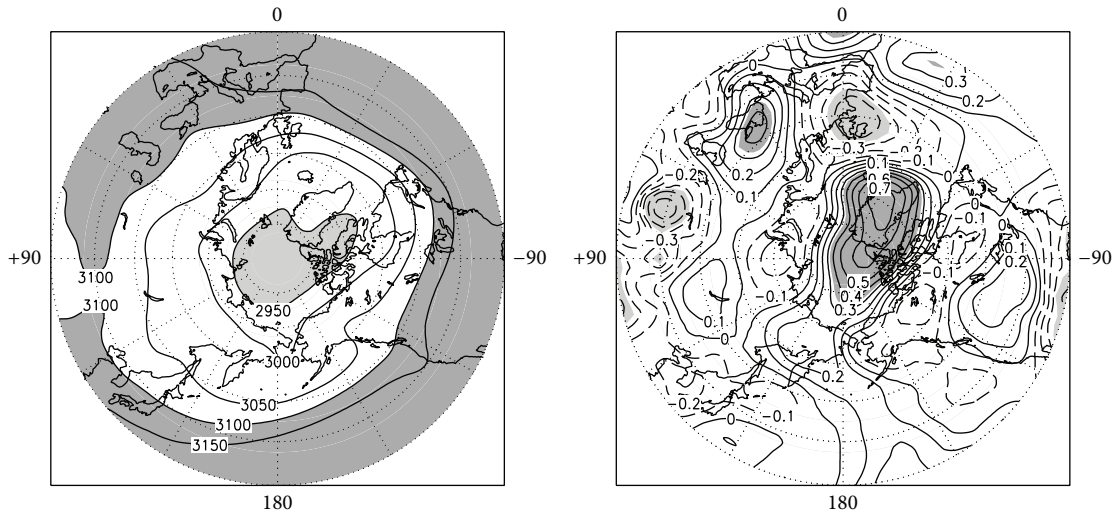

(c) Average H700 in July

(d) H700 in Jul/JJ SIE

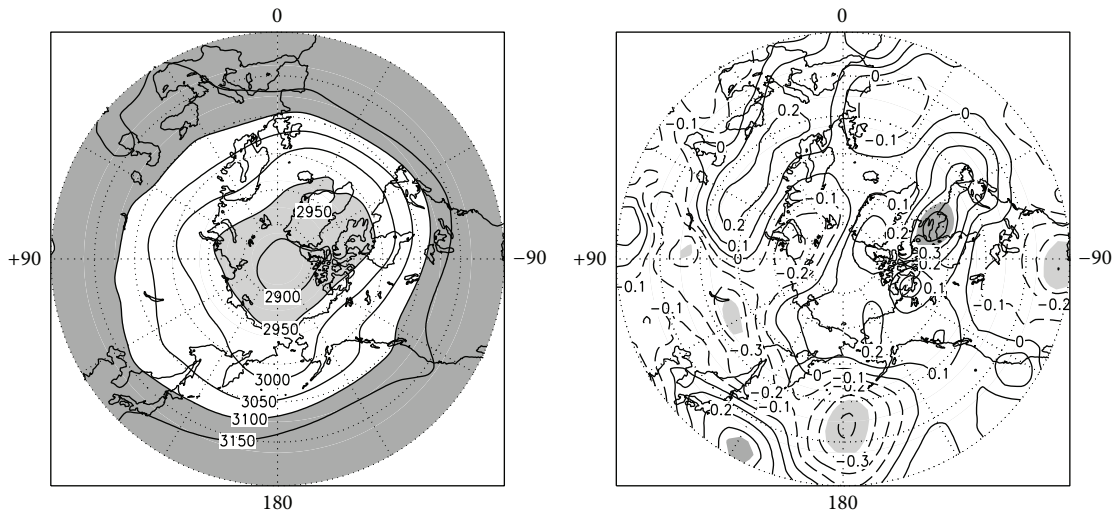

(e) Average H700 in Aug

(f) H700 in Aug/JA SIE

Figure 4: As in Figure 3 but for monthly 700 hPa GHT.

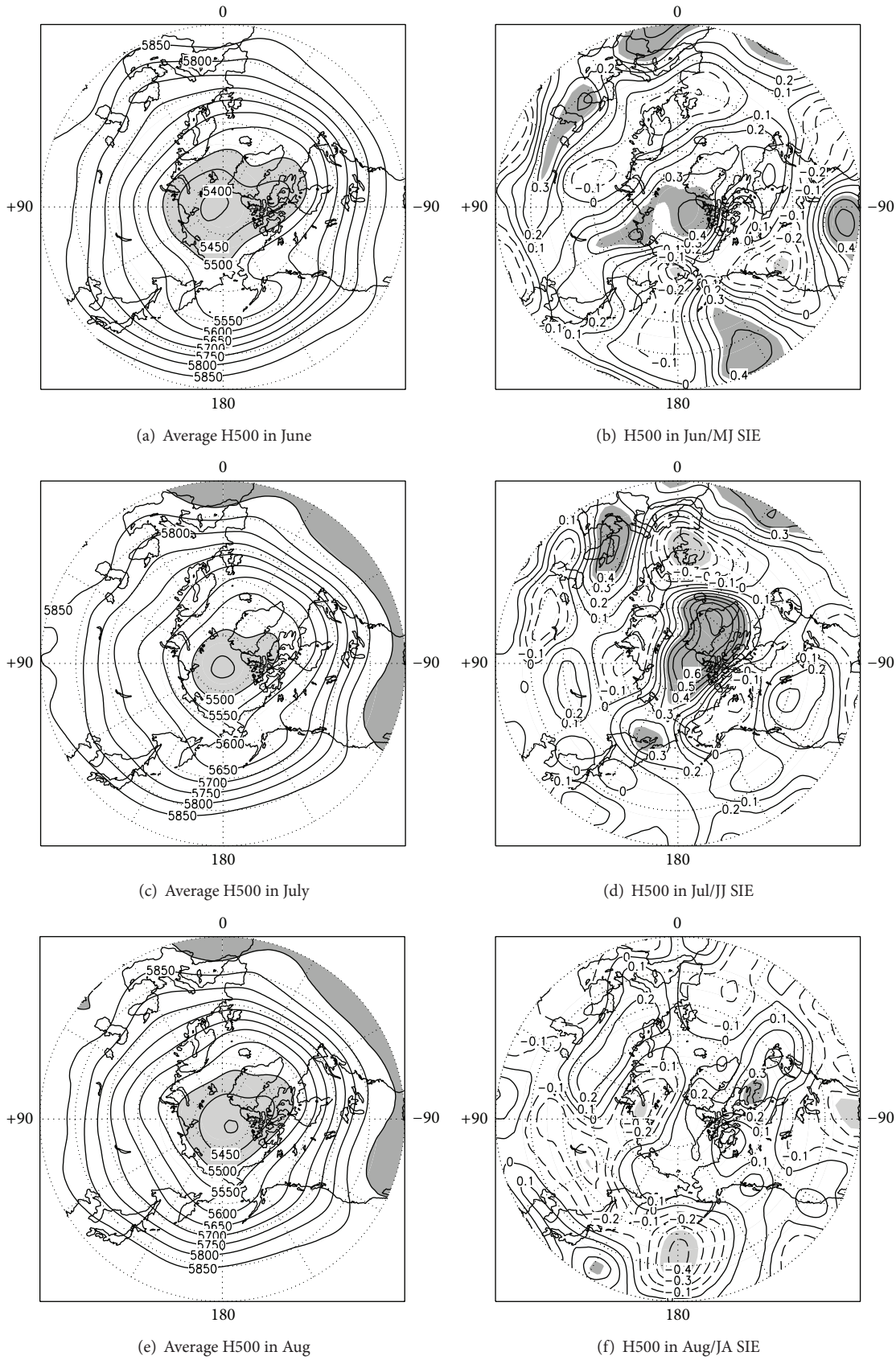

(a) Average H500 in June

(b) H500 in Jun/MJ SIE

(c) Average H500 in July

(d) H500 in Jul/JJ SIE

(e) Average H500 in Aug

(f) H500 in Aug/JA SIE

Figure 5: As in Figure 3 but for monthly 500 hPa GHT.

implies a monthly reduction in Arctic sea ice from June to July is characterized by the enhanced sea level pressure over polar regions in association with more stable weather processes in July.

From the association of the MJ, JJ, and JA with the atmosphere circulation patterns at SLP, 700 hPa, and 500 hPa height, we understand that the JJ has more significant correlation connecting to atmosphere circulation anomalies in polar regions than those for MJ and JA. Annually, the JJ and JA SIE contributed to the decline of SIE in September have the same order of magnitude, but the correlation relationship of large-scale atmosphere circulation anomalies with the JJ is much stronger than that with the JA. It is evident that JA SIE variability was partly affected by large-scale atmosphere circulation anomalies over high latitudes of the western Atlantic sector in August, but the other factors such as the ocean heat flux convergence, local storms, and mesoscale surface winds could be more important (e.g. [26, 44]). Furthermore, while detrending the JJ and JA and the SLP, 700 hPa, and 500 hPa GHT, it is found that their significant correlation modes of the two monthly SIE differences with SLP, 700 hPa, and 500 hPa height fields can be maintained as before (Figure 6).

Figure 7 displays the extreme case analyses for the 10 highest and the 10 lowest JJ and JA SIE during 1979–2012 in association with the anomaly distribution of the SLP field. The 30 yr (1981–2010) averaged SLP in July (Figure 7(a)) and August (Figure 7(b)) exhibits three centers; that is, the midlatitude North Pacific, the Azores High in midlatitudes over North Atlantic, and a Low in midhigh latitudes over Eurasian continent. The SLP departures exceed +3 hPa (from the 30 yr (1981–2010) mean) over the polar regions during July for the 10 highest JJ SIE cases during 1979–2012, whereas the negative anomalies are mainly located in high latitudes from 45°W to 120°E where the departure is lower than −1 hPa (Figure 7(c)). In contrast, for the 10 lowest cases of the JJ SIE, it is characterized (Figure 7(e)) by anomalous low SLP (under −2 hPa) occurring broadly across the Arctic, and positive anomalies (the departure is higher than +1 hPa) are located in midlatitudes over western Europe and eastern Atlantic. Therefore, while positive (negative) SLP anomalies in July occur in polar regions and negative (positive) anomalies in midlatitudes over eastern Atlantic and western Europe, the SLP field anomalies are used to be favourable for more (less) Arctic sea ice melt from June to July. Moreover, the Student's t-test shows that the SLP field anomalies in the polar region and midlatitudes over eastern Atlantic for the 10 highest and 10 lowest JJ SIE cases were all at confidence level of 99% (Figure 7(g)). This result corresponds to significant correlation distributions as shown in Figure 3(d).

Unlike the JJ SIE, the JA SIE connecting to the SLP anomalies is mainly located in polar region along 45°–90°W and high latitudes over western Atlantic and midlatitudes over North Pacific; however, it is weaker than that for JJ SIE cases. For example, the two anomaly areas of the SLP under the 10 highest JA cases are mainly located in the polar region along 45°–90°W where a positive departure is higher than +1 hPa and midlatitudes over North Pacific where a negative departure is lower than −1 hPa (Figure 7(d)). For the 10 lowest JA cases (Figure 7(f)), it shows an opposite anomaly pattern in polar regions along 25–115°W where a negative departure is lower than −1 hPa. The most significant SLP anomalies for extreme JA cases is identified to be north of 60°N along 45°–90°W over western Atlantic (Figure 7(h)). Figure 8 displays the anomalies at 500 hPa GHT field connecting to the JJ and JA extreme cases, and it is found that the July height anomalies at 500 hPa connecting to the extreme JJ cases have similar patterns with the SLP fields except for midlatitudes 30°E over Europe (Figure 8(h)). Particularly, the anomaly patterns at SLP and 500 hPa height in 2007 and 2012 are examined in order to understand extreme situations for sea ice melt. Figure 9 shows anomaly distributions of SLP and height fields at 500 hPa in July and August in 2007 and 2012 relative to the 30 yr mean field. For example, the stronger positive anomalies of SLP occurred in polar regions and high latitudes over eastern Atlantic during July in 2007 and 2012. While comparing the two positive anomaly distribution for SLP in 2007 and 2012, it is noted that the former is higher than the latter. Apparent negative SLP anomalies in July are mainly located in midhigh latitudes along Atlantic and Eurasian continent; however it is noted that there is different anomaly distribution over North Pacific in 2007 with a negative anomaly centered in 40–50°N, 150°W and in 2012 with a positive anomaly centered in 40–50°N, 170°E. Moreover, the 500 hPa height fields also exhibit a similar pattern (Figures 9(e) and 9(f)).

For the two extreme cases in August, the anomaly patterns of SLP are characterized by apparent positive anomalies (higher than +6 hPa) in polar regions and negative anomalies (under −2.5 hPa with light gray shaded in Figures 9(c) and 9(d)) in high latitudes over Eurasian continent and North Pacific. From this analysis, we understand that persistent (July and August) positive anomalies over polar regions and negative anomalies in high latitudes over Eurasian continent in summer are conducive to accelerated ice melting.

3.3. Monthly SIE Differences for JJ and JA and Sea Surface Temperature (SST) Anomalies. The sea surface temperature (SST) plays important roles in climate systems by reemergence mechanism and ocean-atmosphere interaction [45–47]. Local ocean-atmosphere interaction in the North Pacific and North Atlantic is dominated by the forcing of the atmospheric internal variability on SST [48, 49]. Liu et al. [50] pointed out that the Maximum Covariance Analysis suggests a significant local atmospheric response, with the summer atmosphere corresponding to the preceding winter sea surface temperature over the North Pacific based on the observations.

Further analyses on JJ and JA SIE in connection to sea surface temperature (SST) in preceding winter (DJF) and spring (MAM) show that there are slight seasonal differences in correlation between the JJ SIE and the SST over North Pacific and Atlantic in winter and spring (Figure 10). For example, there are three significant correlation centers in preceding winter in the Pacific sector; the first positive center is located in midlow latitudes over central Pacific 20°–40°N, 160°E–150°W, the second positive center is along the coast of East Asia from low to middle latitudes, and the third (a

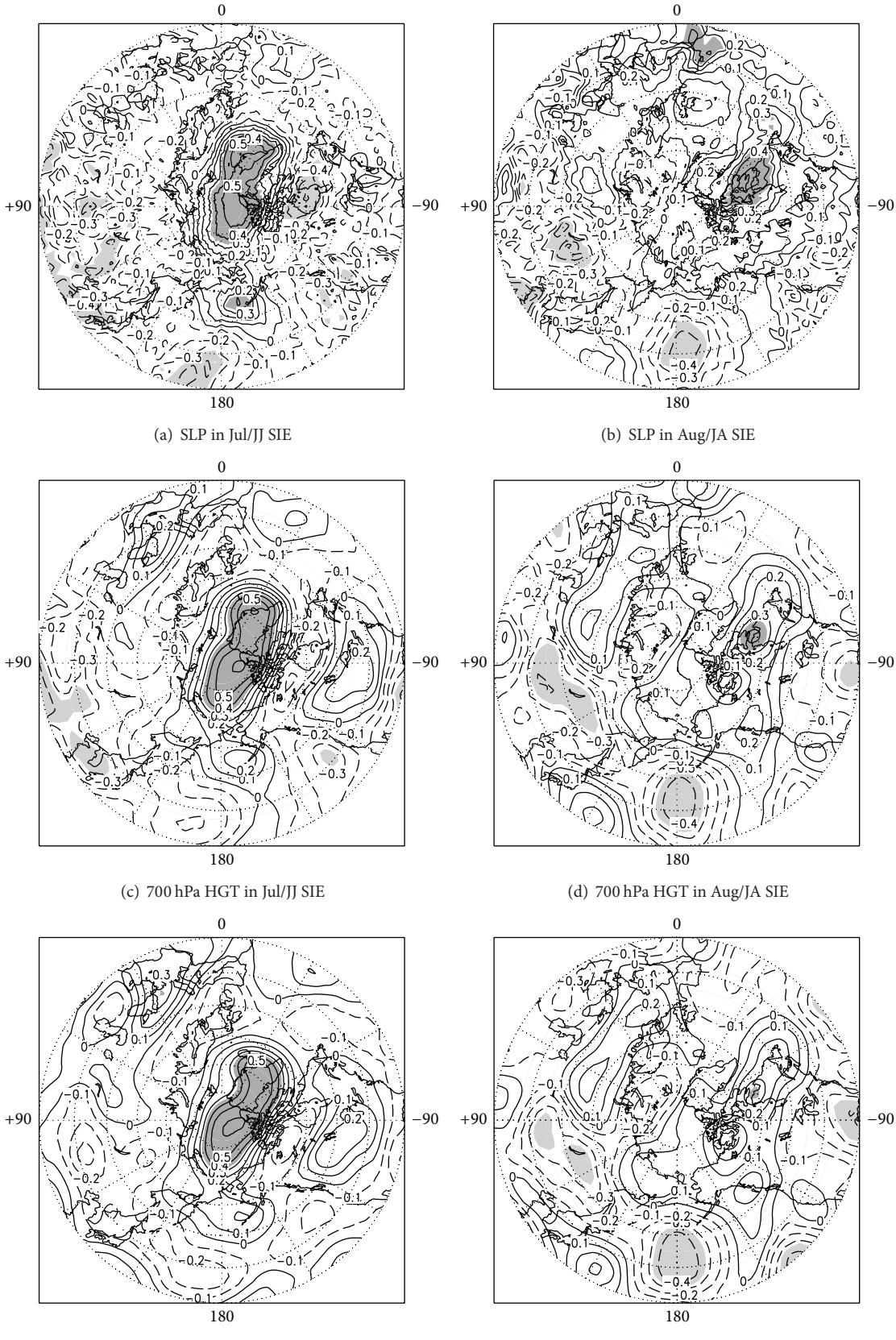

(a) SLP in Jul/JJ SIE

(b) SLP in Aug/JA SIE

(c) 700 hPa HGT in Jul/JJ SIE

(d) 700 hPa HGT in Aug/JA SIE

(e) 500 hPa HGT in Jul/JJ SIE

(f) 500 hPa HGT in Aug/JA SIE

Figure 6: The correlation distribution between monthly surface level pressure (SLP) and 700 hPa and 500 hPa GHT over the north of 30°N in July and August and the monthly SIE differences for the JJ and JA after detrending: (a) July SLP and JJ SIE, (b) August SLP and JA SIE, (c) July 700 hPa GHT and JJ SIE, (d) August 700 hPa GHT and JA SIE, (e) July 500 hPa GHT and JJ SIE, and (f) August 500 hPa GHT and JA SIE.

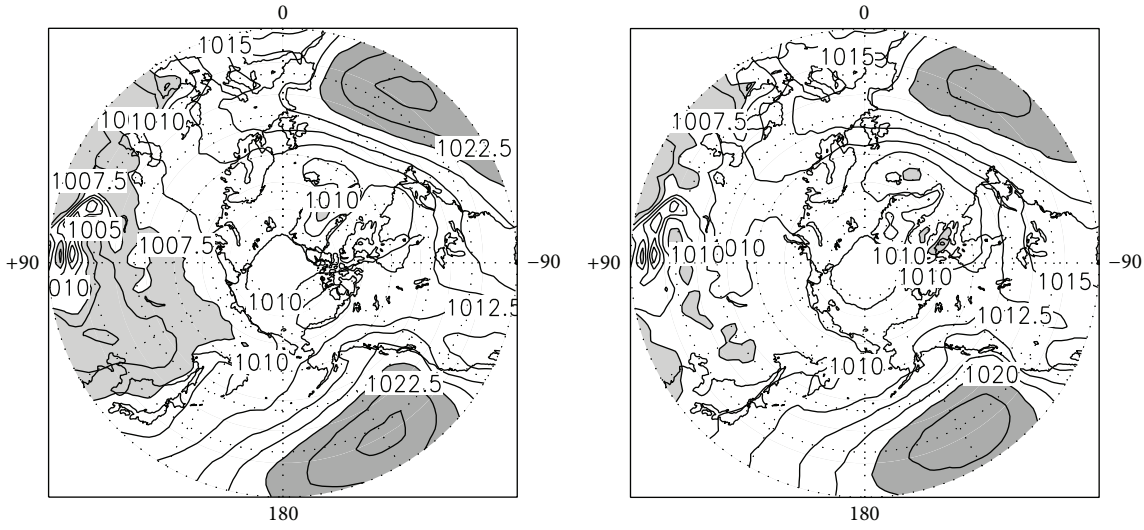

(a) 30 yr SLP (Jul)

(b) 30 yr SLP (Aug)

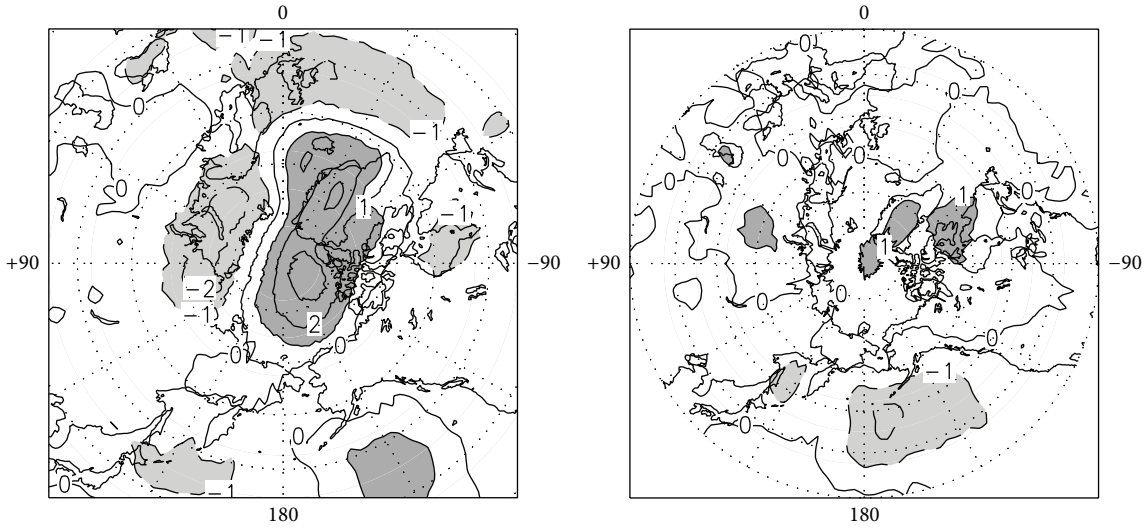

(c) High JJ case

(d) High JA case

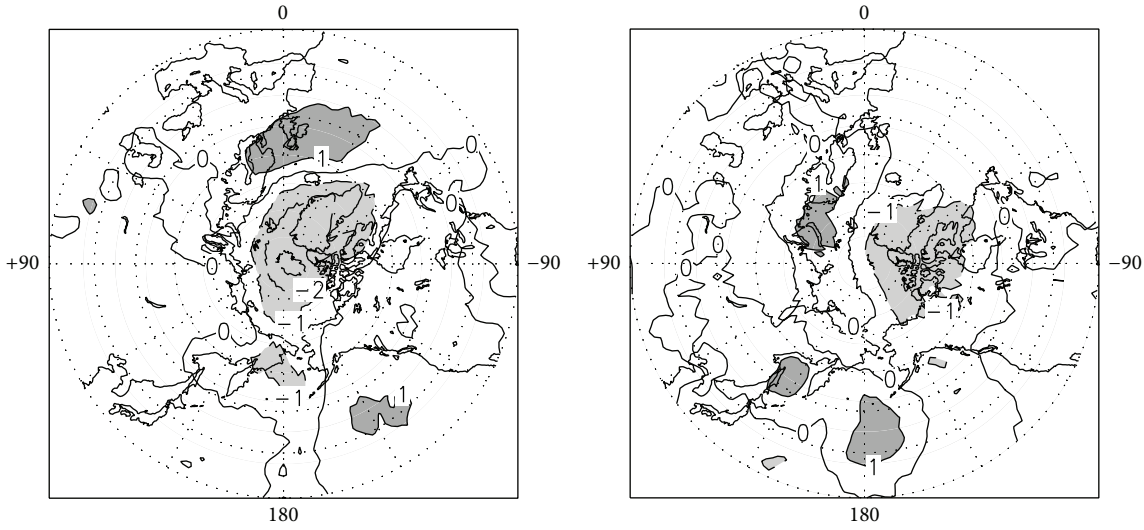

(e) Low JJ case

(f) Low JA case

Figure 7: Continued.

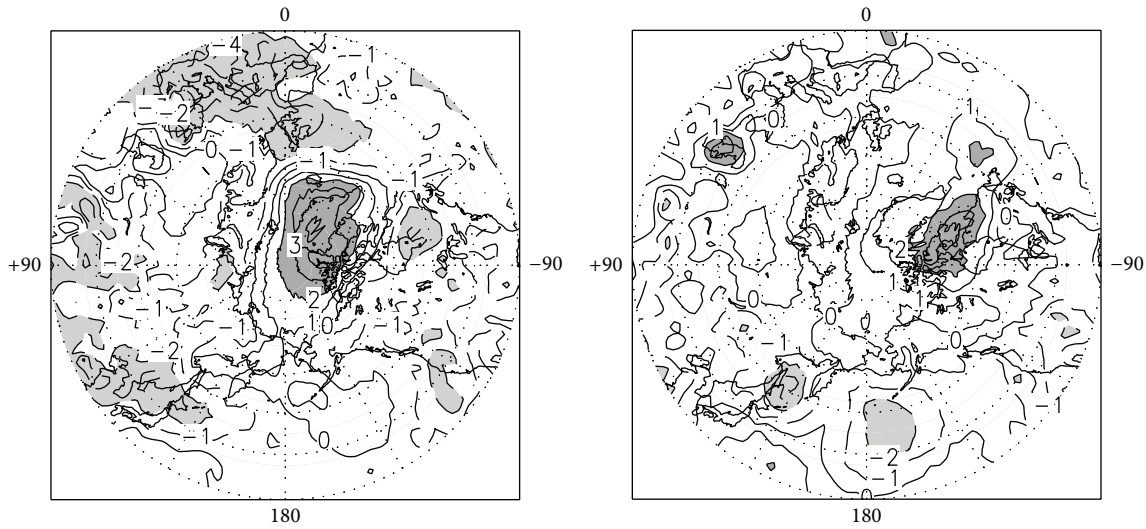

(g) t-test for JJ (h) t-test for JA

Figure 7: The anomaly distributions of SLP in July and August and their associations with the 10 highest and 10 lowest JJ and JA SIE cases over the north of 30°N: (a) a 30 yr SLP average in July for 1981–2010, (b) a 30 yr SLP average in August for 1981–2010, (c) departure of average SLP in July for the 10 highest JJ SIE cases relative to the 30 yr average SLP in (a), (d) departure of average SLP in August for the 10 highest JA SIE cases relative to the 30 yr average SLP in (b), (e) as in (c) but for the 10 lowest JJ SIE cases, (f) as in (d) but for the 10 lowest JA SIE cases, (g) Student's t-test scores of SLP in July for 10 highest and 10 lowest JJ SIE cases, and (h) as in (g) but in August for 10 highest and 10 lowest JA SIE cases.

negative center) is along the subtropical regions over central-eastern North Pacific to the middle latitudes of the western coastal regions over North America. In the Atlantic sector, there are two positive correlation centers located in midlow latitudes over Atlantic and the polar region.

Meanwhile, it is noted that the positive correlation areas in spring are concentrated to central Pacific with the significant areas located in 30°–50°N, 160°E–160°W and much significant negative center (negative correlation coefficient is less than −0.5) is located in 20°–30°N, 120°–150°W, a subtropical eastern North Pacific. The positive correlation of the SST in preceding winter and spring with JJ SIE at above 95% confidence levels also exists in polar regions and middle latitudes over Atlantic (Figures 10(a) and 10(c)).

Figure 11 shows the distribution of SST in spring and climatologic features with the extreme JJ SIE cases. The 30 yr average SST (1981–2010) in spring (MAM) over the north of 10°N is shown in Figure 11(a), ranging from lower than 0°C in the Arctic (light gray shaded) to higher than 27.5°C (gray shaded) over tropical regions. Figures 11(b) and 11(c) depict the SST anomaly distributions for the 10 highest and 10 lowest JJ SIE cases, respectively. For the 10 highest JJ SIE cases, the warmest anomaly center is +0.5°C higher than the 30 yr average located in midlatitudes over central North Pacific; and the second warmest anomaly center is higher than +0.3°C mainly located in polar region (30°W) over Atlantic. Meanwhile, one cold anomaly center is lower than −0.4°C located in subtropical eastern North Pacific (20°–30°N) along the western coast of North America. In contrast, for the 10 lowest JJ SIE cases, opposite anomaly distribution patterns of the SST in spring were observed. Furthermore, Student's t-test (Figure 11(d)) show that the SST anomalies for the above-referenced warm and cold centers during the 10 highest and 10 lowest JJ SIE cases are all at 99% confidence level. This result implies that the preceding winter and spring SST in midlatitude in North Pacific and Atlantic maintain the persistence significant correlation with the JJ SIE. Particularly, the SST anomalies in spring over the North Pacific and Atlantic, shown in Figure 10(c), are significantly correlated to the JJ SIE in the three regions over midlatitudes in North Pacific and Atlantic, that is, 30°–50°N, 160°E–160°W (Area 1) (central North Pacific), 20°–30°N, 120°–150°W (Area 2) (eastern North Pacific), and 25°–35°N, 20°–45°W (Area 3) (North Atlantic). Furthermore, the SSTs in the three areas in spring are averaged as the SST indices to analyze their connection with the JJ SIE, SIE in September, and summer atmosphere circulation patterns at 500 hPa height field. Table 2 shows the relationships of the three SST indices with the JJ SIE and the SIE in September, which have quite significant confidence level of 99%. The correlation between SST index I (Area 1) and SIE in September is the most significant (its coefficient is −0.603). Figure 12 shows lag correlation distributions between the spring SST indices and summer 500 hPa height fields. It is found that there are significant correlations of the three SST indices with the atmosphere circulation in summer (JJA) over polar regions (Figures 12(a), 12(c), and 12(e)). For the SST index averaged in 30°–50°N, 160°E–160°W, there is different distribution with 500 hPa height field in polar region during JJA and JAS, respectively; relatively, the pattern in JJA is more important. For the other two SST indices in 20°–30°N, 120°–150°W and 25°–35°N, 20°–45°W, they have similar correlation patterns in

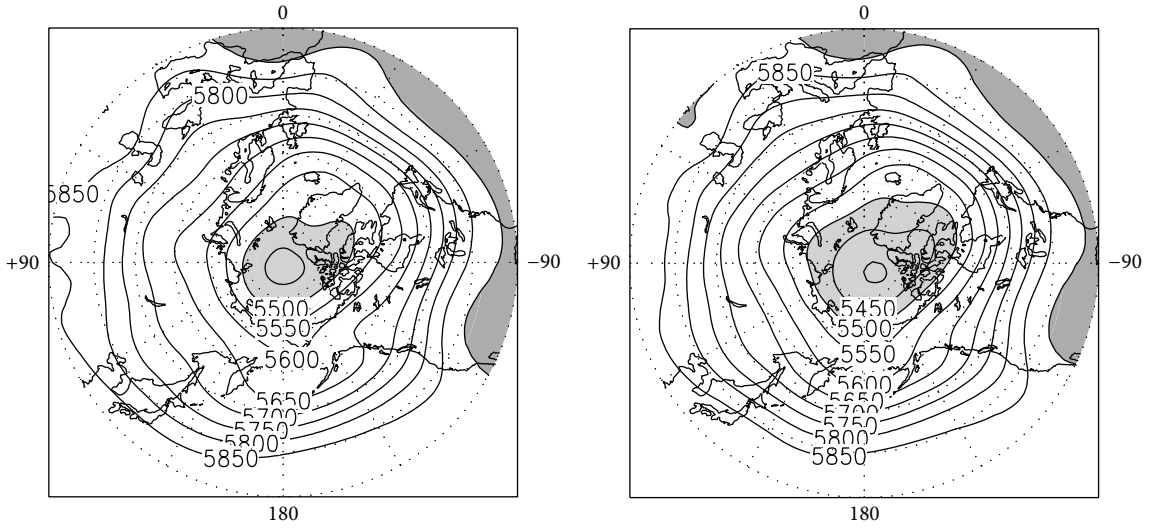

(a) 30 yr H 500 hPa (Jul)

(b) 30 yr H 500 hPa (Aug)

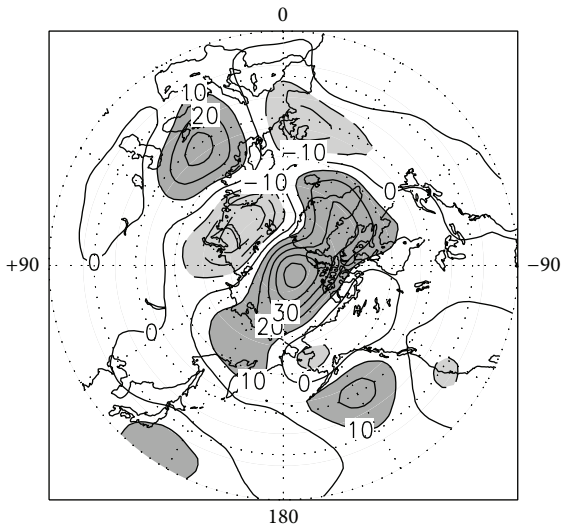

(c) High JJ case

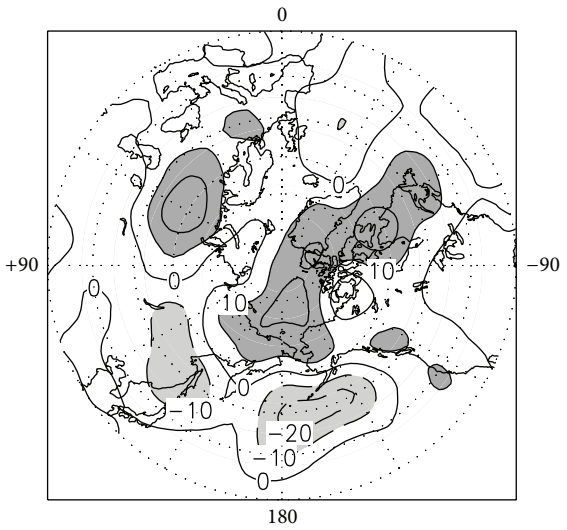

(d) High JA case

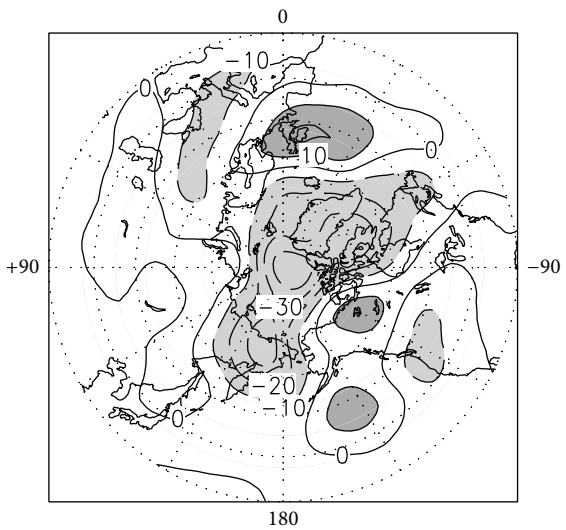

(e) Low JJ case

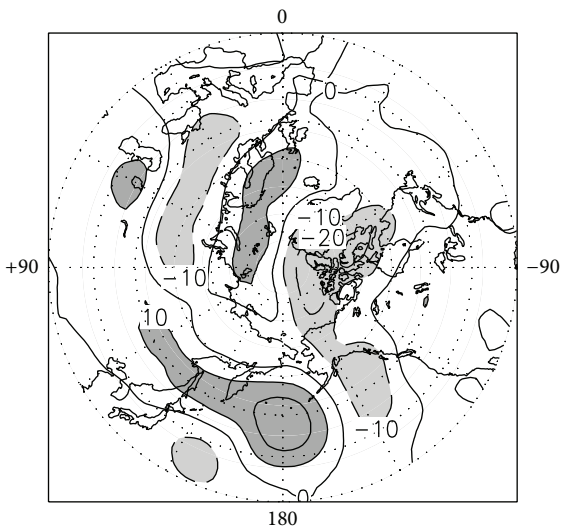

(f) Low JA case

Figure 8: Continued.

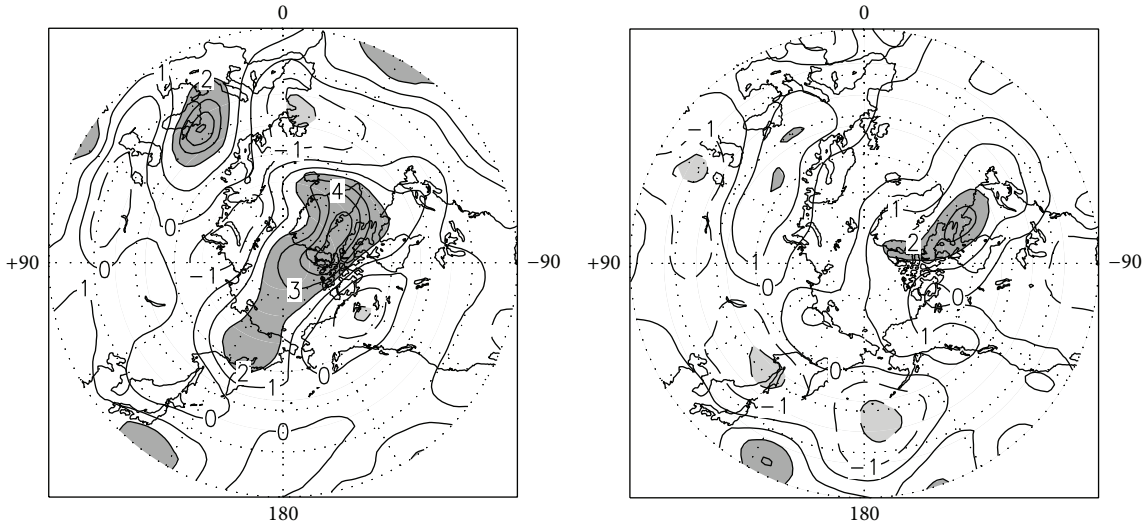

(g) t-test for JJ (h) t-test for JA

Figure 8: As in Figure 7 but for monthly 500 hPa GHT.

Table 2: The list of correlation relations between SST indices and the JJ SIE or SIE in September for 1979–2012. Note: Index I is SST averaged in 30°–50°N, 160°E–160°W, Index II is SST averaged in 20°–30°N, 120°–150°W, and Index III is SST averaged in 25°–35°N, 20°–45°W. The 99% confidence level is 0.435.

SST index	JJ SIE	SIE in Sept
Index I	0.477	−0.603
Index II	−0.561	0.527
Index III	0.570	−0.552

JJA and JAS, but the latter (JAS) become more significant in polar regions and midlow latitudes over North Pacific. This analysis implies that the spring SSTs in midlatitudes over North Pacific and Atlantic have significant lag-correlation with summer atmosphere circulation at 500 hPa height fields in polar regions.

In contrast, there is not significant correlation between the JA SIE and the SST in the preceding winter and spring except for two small regions in midlatitudes over central North Pacific and polar regions along 60°–100°W (Figures 10(b) and 10(d)). Why are monthly changes of sea ice extent (SIE) for JJ and JA over Arctic so different in association with large-scale atmosphere and ocean circulations? Bitz et al. [44] pointed out that absorbed solar radiation is the largest component of the ocean energy budget at high latitudes while the ocean heat flux convergence plays an important role in variations of sea surface temperature which has a relatively small annual variation range. Besides the influence from atmospheric-oceanic large-scale circulation, local surface wind, storm track, and ocean heat flux which may have a more important effect on the variability of the JA SIE. From the above analysis, we conclude that atmospheric circulation anomalies in July exert a stronger influence upon JJ SIE than the other monthly differences of SIE in warm season.

3.4. The Monthly SIE Difference and the SIE in September and Large-Scale Atmospheric Circulation Indices. Table 3 shows the correlation analyses of NAO index (NAOI) and AO index (AOI) with the JJ, JA, and the September SIE for both original and detrended time series. The NAOI in June has the most significant correlation with the JJ and the SIE in September, −0.521 (−0.433 after detrending) and 0.444 (0.342 after detrending), separately. When the NAOI is in a positive phase, the pressure difference of the Icelandic low and the Azores high is large, and the northeastern Atlantic experiences increased storminess [38, 51]. In contrast, the negative NAOI phase shows a weak subtropical high and a weak Icelandic low. It is noted that NAOI in July has significant negative correlation with the JJ, and its correlation coefficient is −0.508 at confidence level of 99%, which corresponds to a positive anomaly over polar region and a negative anomaly in midlatitudes over eastern Atlantic. As mentioned in Figures 3(d) and 7, it is identified that the dipolar behavior of July SLP connecting to the JJ SIE corresponds to a negative phase of NAO in June and July, respectively. On the other hand, it is notable that the JA has a positive correlation with NAOI in March at confidence level of 95% for original data (0.358) and detrended (0.389). Obviously, there is quite a different association of NAOI with the JJ and JA SIE.

Meanwhile, the relationship of AOI in June and July associated with the JJ is also examined, with negative correlation coefficients −0.427 and −0.377, separately. When pressure is high in the Arctic and low in midlatitudes, the Arctic Oscillation is in its negative phase. From this result, it is noted that the correlation of AOI with the JJ is lower than that simultaneous NAOI (Table 3). AOI in April has a positive significant correlation with the JJ but this did not happen in simultaneous NAOI. Particularly, AOI in March connected to the JA shows a much better confidence level (their correlation coefficient is 0.513 (original) and 0.498 (detrended), separately) than the simultaneous NAOI. However, the physical

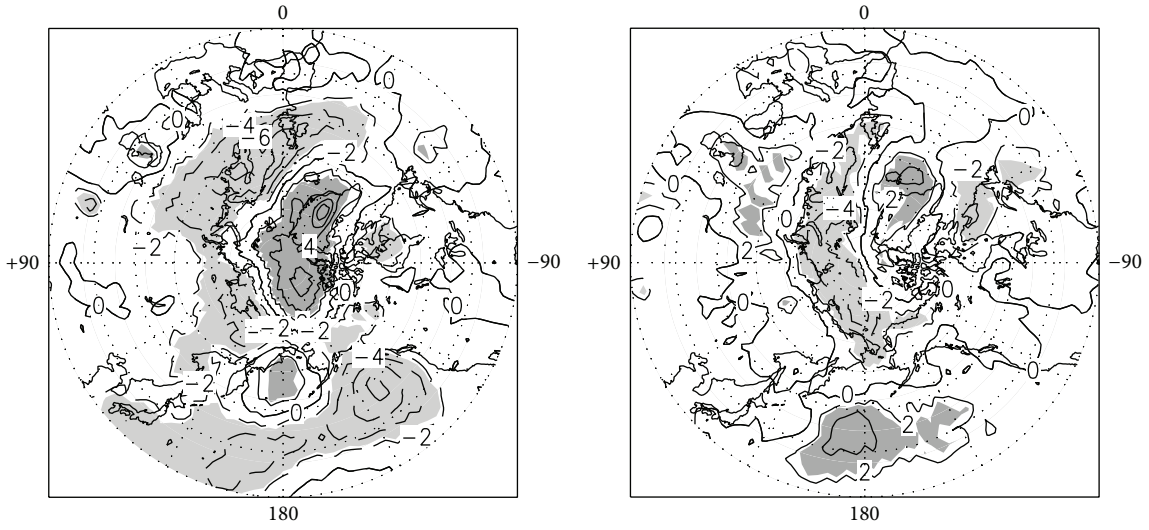

(a) SLP 2007 (Jul)

(b) SLP 2012 (Jul)

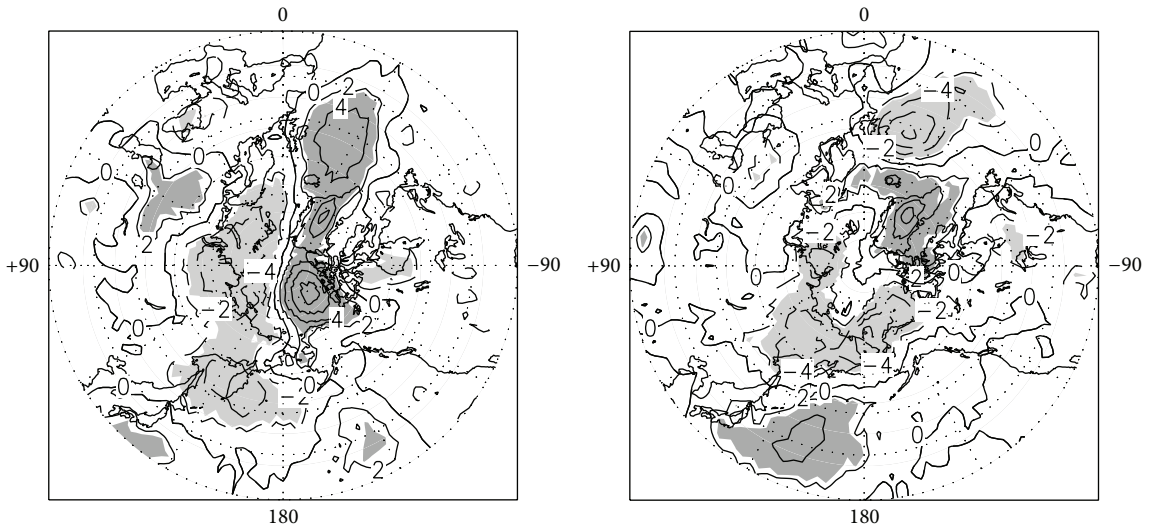

(c) SLP in 2007 (Aug)

(d) SLP 2012 (Aug)

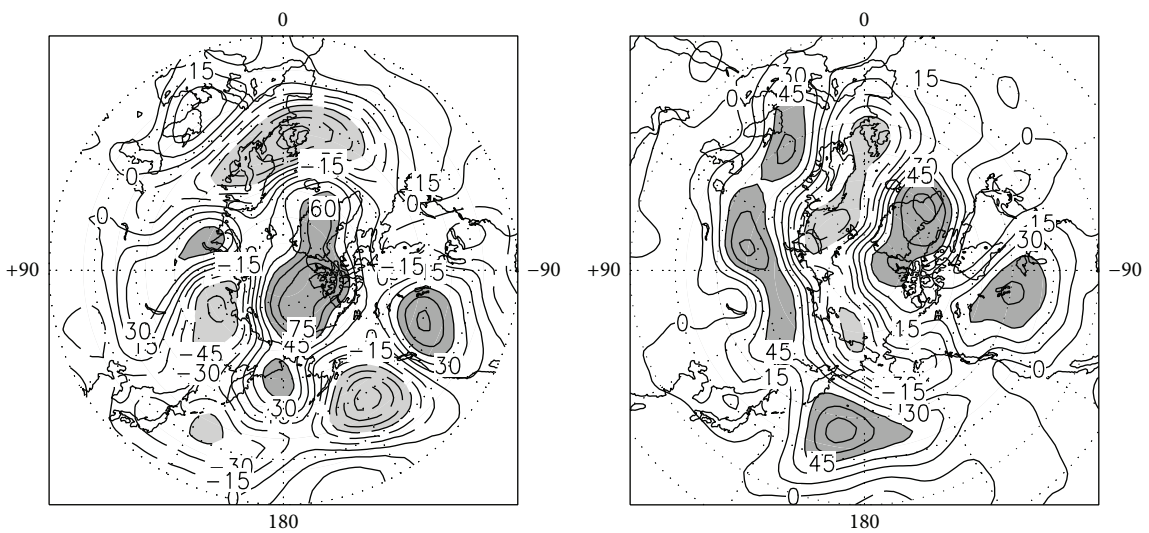

(e) H500 in 2007 (Jul)

(f) H500 in 2012 (Jul)

Figure 9: Continued.

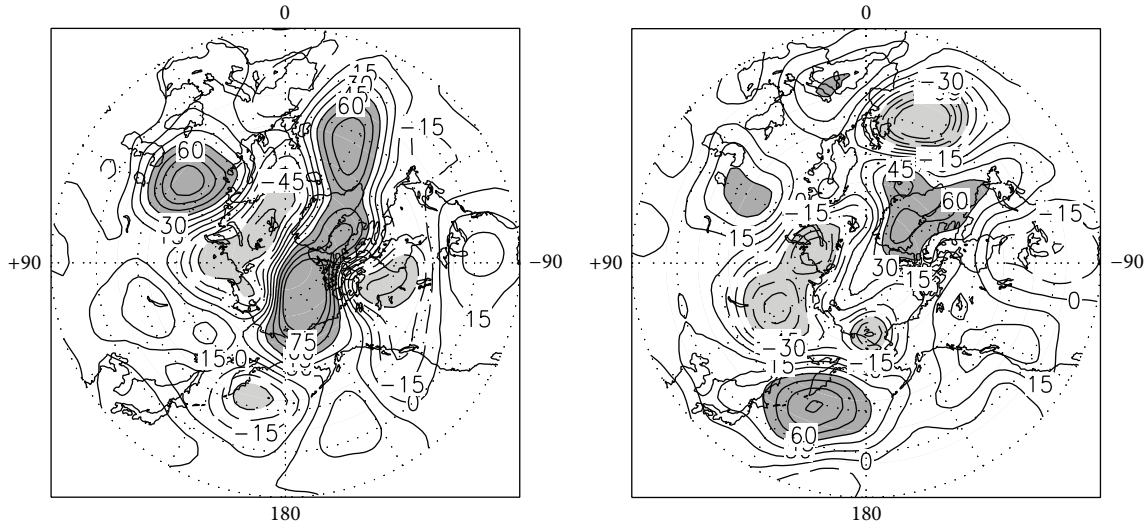

(g) H500 in 2007 (Aug) (h) H500 in 2012 (Aug)

Figure 9: The anomalies at SLP and 500 hPa HGT in July and August for 2007 and 2012 cases: (a) the July SLP anomaly in 2007 relative to the 30 yr (1981–2010) average July SLP, (b) as in (a) but for 2012, (c) the August SLP anomaly in 2007 relative to the 30 yr (1981–2010) average August SLP, (d) as in (c) but for 2012, (e) the July 500 hPa GHT anomaly in 2007 relative to the 30 yr (1981–2010) average July 500 hPa GHT, (f) as in (e) but for 2012, (g) the August 500 hPa GHT anomaly in 2007 relative to the 30 yr (1981–2010) average August 500 hPa GHT, and (h) as in (g) but for 2012.

Table 3: Correlation analyses of the September SIE, the JJ and JA SIE with monthly NAO and AO index from 1979 to 2012. Note: correlation coefficients higher than 0.339 and 0.435 are defined as confidence levels at 95% (∗5) and 99% (∗1), respectively.

Index	SIE\monthly index	Jan	Feb	Mar	Apr	May	June	July	August	Sept
NAO	SIE in Sept	−0.091	0.085	−0.019	−0.046	0.203	**0.444**^{*1}	**0.497**^{*1}	**0.351**^{*5}	−0.201
	After detrending	−0.027	0.018	−0.193	0.038	0.250	**0.342**^{*5}	0.263	0.101	**−0.339**^{*5}
	JJ SIE	−0.139	−0.118	−0.077	0.098	−0.121	**−0.521**^{*1}	**−0.508**^{*1}	−0.326	0.190
	After detrending	−0.250	−0.080	−0.022	0.064	−0.087	**−0.433**^{*5}	−0.334	−0.145	0.222
	JA SIE	0.108	0.160	**0.358**^{*5}	0.236	−0.015	−0.189	−0.003	−0.041	0.176
	After detrending	0.092	0.184	**0.389**^{*5}	0.226	0.003	−0.129	0.103	0.038	0.175
AO	SIE in Sept	−0.107	−0.027	−0.250	−0.285	−0.036	0.312	0.237	0.237	−0.236
	After detrending	−0.128	−0.075	−0.236	−0.257	0.094	0.249	0.179	0.160	−0.161
	JJ SIE	−0.008	−0.012	0.034	**0.419**^{*5}	0.041	**−0.427**^{*5}	**−0.377**^{*5}	−0.301	0.213
	After detrending	−0.048	−0.023	−0.077	**0.400**^{*5}	−0.027	**−0.382**^{*5}	**−0.352**^{*5}	−0.245	0.132
	JA SIE	0.245	0.165	**0.513**^{*1}	0.084	0.122	−0.125	0.031	−0.095	0.199
	After detrending	0.240	0.167	**0.498**^{*1}	0.048	0.103	−0.082	0.070	−0.059	0.167

mechanism of the JA associated with NAOI or AOI in March is not clear. While comparing the relationship of preceding NAOI and AOI with the SIE in September, it is noted that NAOI in June has a better relationship to the loss of Arctic sea ice in September than AOI (Table 3).

3.5. Forecasting the September SIE Based on Leading Monthly SIE Differences. Based on the above analysis, we understand that the variations of September SIE is closely related to preceding monthly SIE differences for JJ and JA which are connecting to atmosphere-ocean circulation anomalies. Therefore, these two preceding SIE differences (JJ and JA) can be used as prognostic variables, which do not only have a higher correlation with the September SIE but are also almost independent from each other. The two variables are input into the forecasting equation via multiple regression analysis.

A simple multiple regression equation is established using two independent variables $\mathrm{SIE}_{\mathrm{JJ}}$ and $\mathrm{SIE}_{\mathrm{JA}}$ and one dependent variable $\widehat{Y}_t$ in the linear relationship case:

$$\widehat{Y}_t = A_0 + A_1 \cdot \mathrm{SIE}_{\mathrm{JJ}} + A_2 \cdot \mathrm{SIE}_{\mathrm{JA}}, \tag{1a}$$

where $\widehat{Y}_t$ is the predicted value for sea ice extent (SIE) in September and $\mathrm{SIE}_{\mathrm{JJ}}$ and $\mathrm{SIE}_{\mathrm{JA}}$ are the SIE difference for June minus July (JJ SIE) and July minus August (JA SIE), respectively. A_0 is the intercept of Y_t, A_1 and A_2 are multiple regression coefficients. Based on the three time series of JJ, JA

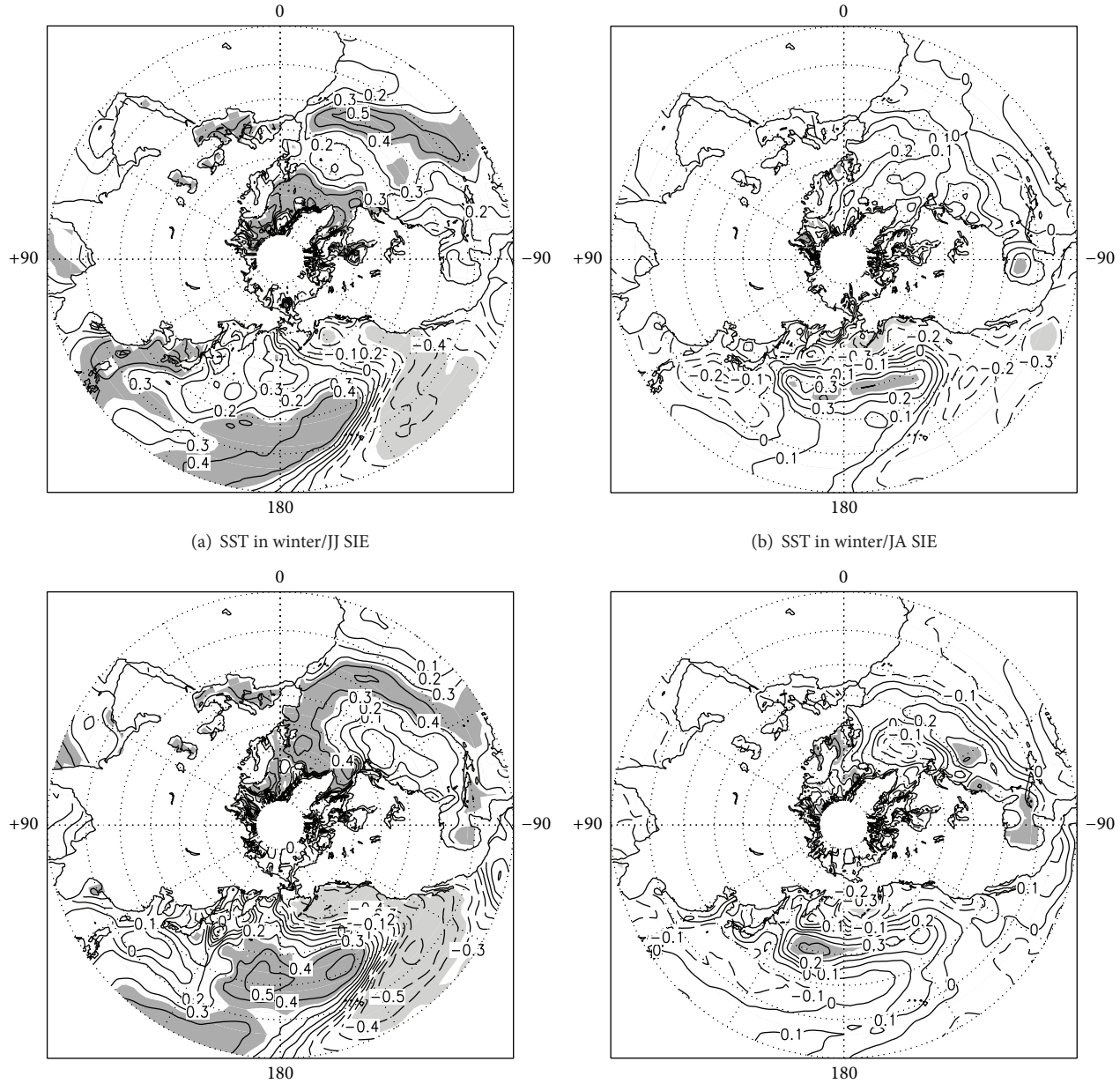

(a) SST in winter/JJ SIE

(b) SST in winter/JA SIE

(c) SST in spring/JJ SIE

(d) SST in spring/JA SIE

Figure 10: The correlation distributions between sea surface temperature (SST) in preceding winter (DJF) and spring (MAM) with SIE difference for JJ and JA over the north of 10°N: (a) SST in winter and JJ SIE, (b) SST in winter and JA SIE, (c) SST in spring and JJ SIE, and (d) SST in spring and JA SIE.

SIE, and the SIE in September for 1979–2012, the following regression equation could be used:

$$\widehat{Y}_t = 14.419 - 1.937 \cdot \mathrm{SIE}_{\mathrm{JJ}} - 1.466 \cdot \mathrm{SIE}_{\mathrm{JA}}. \quad (1b)$$

After detrending the JJ and JA SIE and September SIE, (1a) can be updated as

$$\widehat{Y}_{t-d} = 0.000294 - 1.152 \cdot \mathrm{SIE}_{\mathrm{JJ}-d} - 1.142 \cdot \mathrm{SIE}_{\mathrm{JA}-d}, \quad (1c)$$

where $\widehat{Y}_{t-d}$, $\mathrm{SIE}_{\mathrm{JJ}-d}$, and $\mathrm{SIE}_{\mathrm{JA}-d}$ are the same as (1a) but after detrending, respectively.

Figure 13 shows the time series of the predicted September SIE from (1a) based on original variable data and after detrending in comparison with the satellite observed September SIE during 1979–2014. The predicted curves from (1b) have a better fit to the observed values (Figure 13(a)), and its correlation coefficient with the observed is 0.884. Table 4 shows that the F-statistic value from (1b) is larger (53.21) than that (39.35) from (1c), and much higher than the upper critical value of $F_{\varepsilon=0.01} = 5.36$. Moreover, we understand that the detrended results are equally significant (Table 4) and the

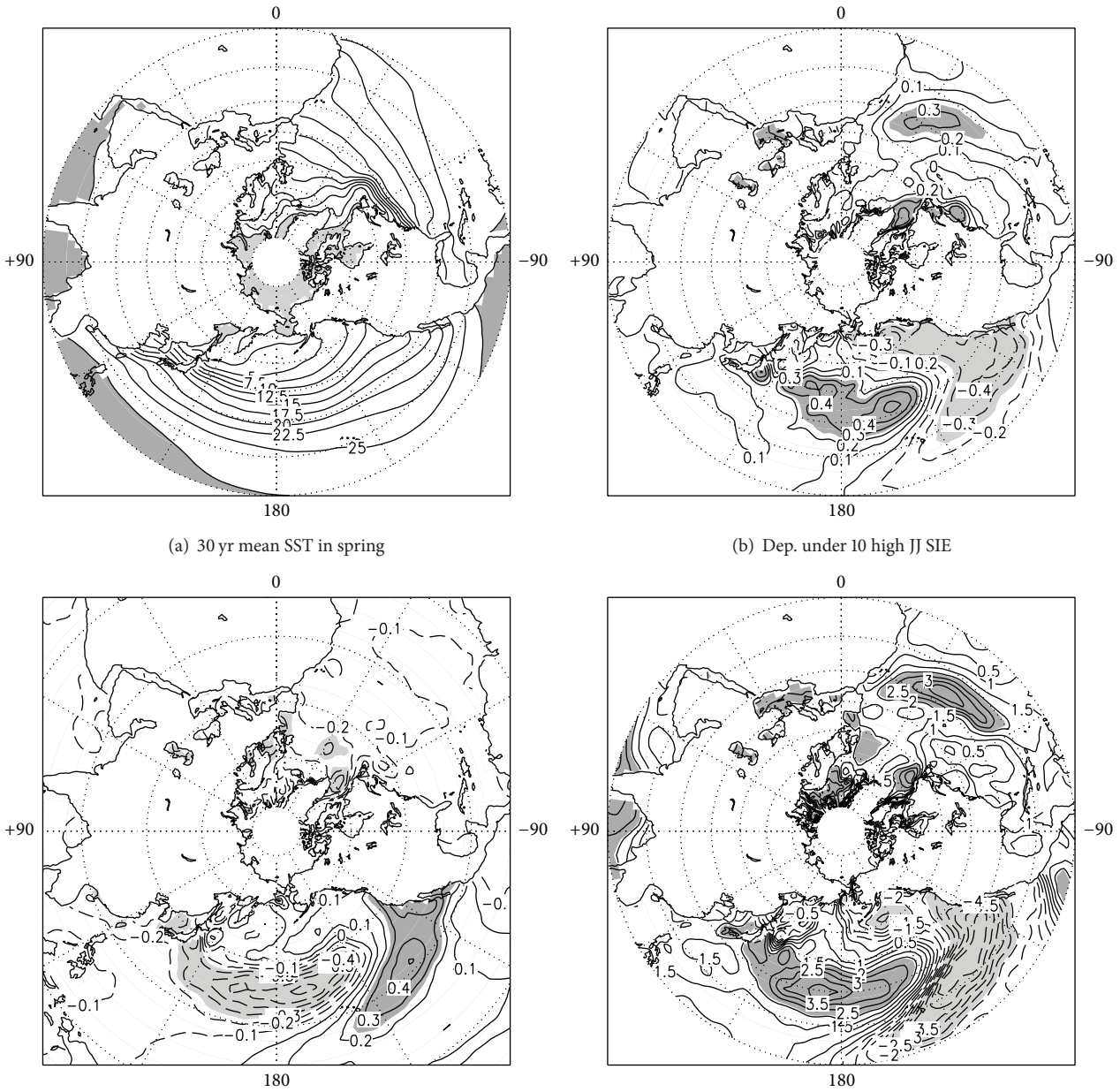

(a) 30 yr mean SST in spring

(b) Dep. under 10 high JJ SIE

(c) Dep. under 10 low JJ SIE

(d) t-test for SST in spring

Figure 11: The distributions of surface sea temperature (SST) in spring (MAM) and its associations with the 10 highest and 10 lowest JJ SIE over the north of 10°N during 1979–2012: (a) a 30 yr average SST in MAM for 1981–2010, (b) departure of average SST for the 10 highest JJ SIE cases relative to the 30 yr average SST in (a), (c) as in (b) but for the 10 lowest JJ SIE cases, and (d) Student's t-test scores of SST for 10 highest and 10 lowest JJ SIE cases.

Table 4: Statistical analyses for the simple forecasting models from (1a); mean absolute percentage error (MAPE) and root mean squared error (RMSE) from (3a) and (3b) are two indictors used to show the feature of the prediction error for Arctic sea ice in September. The critical value of F-test ($F_{\alpha=0.01}$) for (1a) is 5.36.

Type	Predicted equation (1a)	MAPE %	RMSE Mkm^2	Corr. of observed with predicted values	F-statistic values
Original	Predicted value (1b)	6.04	0.5017	0.880	53.21
Detrended	Predicted value (1c)	1.52	0.2949	0.847	39.35

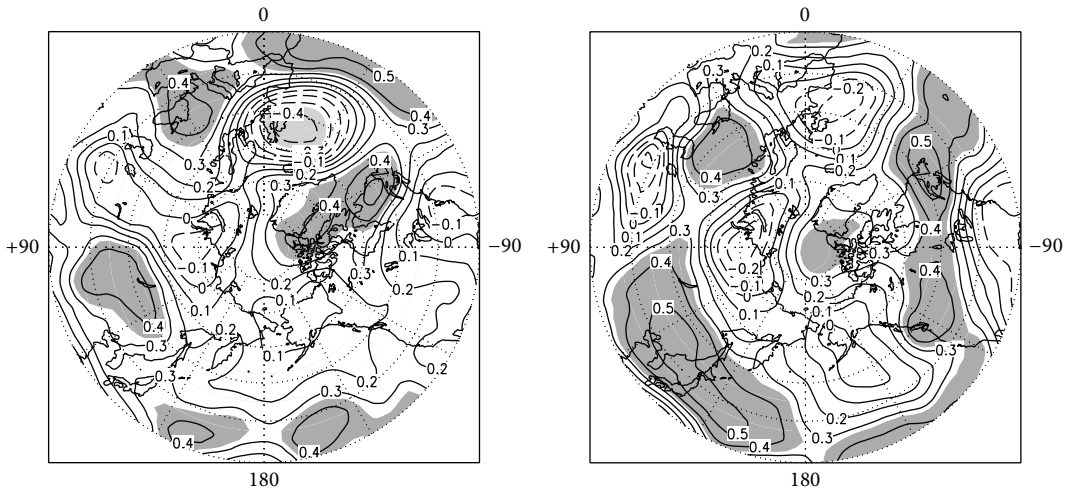

(a) H500 in Jun–Aug/SST-1

(b) H500 in Jul–Sept/SST-1

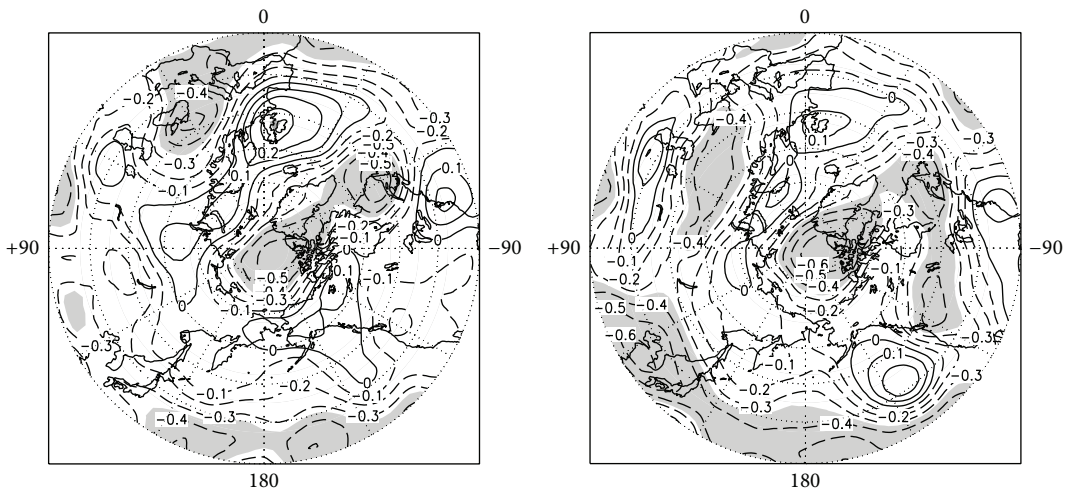

(c) H500 in Jun–Aug/SST-2

(d) H500 in Jul–Sept/SST-2

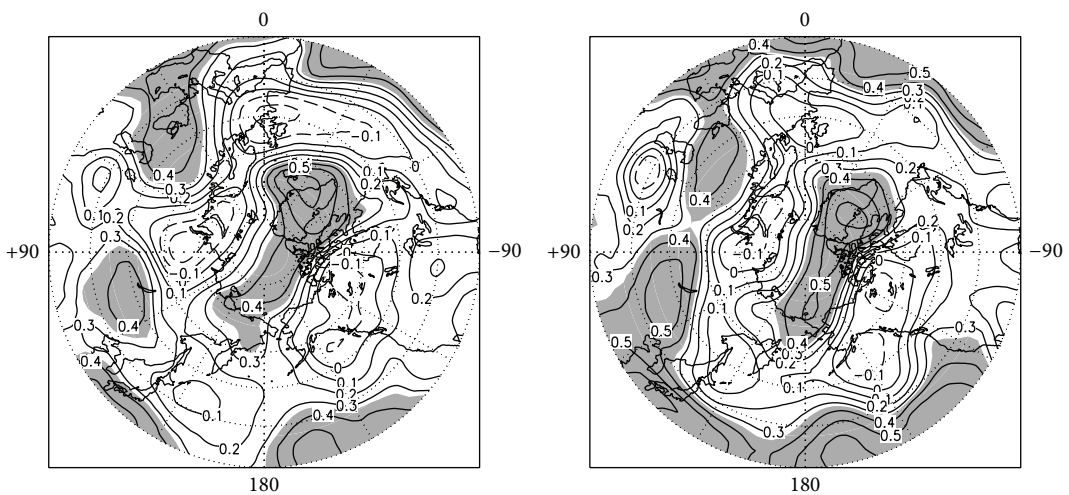

(e) H500 in Jun–Aug/SST-3

(f) H500 in Jul–Sept/SST-3

Figure 12: The correlation distribution between surface sea temperature (SST) indices in spring (MAM) and 500 hPa height (H500) in summer (JJA and JAS): (a) SST index in central North Pacific (30°–50°N, 160°E–160°W) and H500 in JJA, (b) as in (a) but for H500 in JAS, (c) SST index in eastern North Pacific (20°–30°N, 120°–150°W) and H500 in JJA, (d) as in (c) but for H500 in JAS, (e) SST index in midlatitudes over Atlantic (25°–35°N, 20°–45°W) and H500 in JJA, and (f) as in (e) but for H500 in JAS.

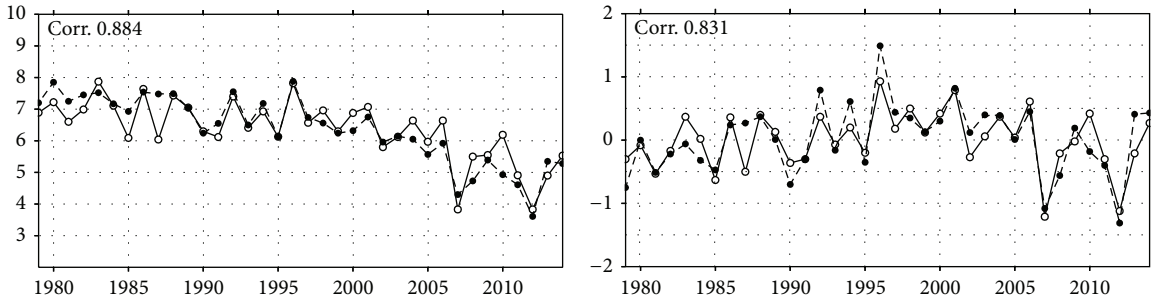

(a) Forecast (solid) by (1b) and Sept SIE (dashed)

(b) As in (a) but for detrended case (1c)

Figure 13: The time series of SIE observed in September and a multiple regression forecasted SIE in September during 1979–2014: (a) the observed versus predicted September SIE based on two variables the JJ and JA SIE and (b) as in (a) but for the variables detrended case.

original is much better. So we chose the original time series to do this prediction for the September SIE.

Furthermore, in order to examine the predictive accuracy for Arctic sea ice, the concept of the forecast error is introduced, which is the difference between the observed and the forecasting value for the corresponding period 1979–2012, and their relationship formula is as follows:

$$E_t = Y_t - F_t, \tag{2}$$

where E_t is the forecast error at time t, Y_t is the actual value at time t, and F_t is the forecast for time t. Here, measures of aggregate error are based on the following two equations.

(1) The mean absolute percentage error (MAPE) is given by

$$\text{MAPE} = \frac{1}{N}\sum_{i=1}^{N}\left|\frac{Y_i - F_i}{Y_i}\right| = \frac{1}{N}\sum_{1}^{N}\left|\frac{E_i}{Y_i}\right|. \tag{3a}$$

(2) Root mean squared error (RMSE) is given by

$$\text{RMSE} = \sqrt{\frac{\sum_{i=1}^{N} {E_i}^2}{N}}. \tag{3b}$$

Table 4 also lists the statistical characteristics for the simple forecasting model from (1b), (1c) from 1979 to 2012. Based on the forecasting equation (1b) and the 2013 and 2014 dataset about JJ (3.13 and 3.02 Mkm^2) and JA (2.36 and 2.03 Mkm^2), the forecasting value for the SIE in September in the two years can be obtained. The results show that the predicted September SIE (unit: Mkm^2) for 2013 is 4.90 Mkm^2 from (1b) and −0.45 Mkm^2 (or −8.4%) lower than the observed 5.35 Mkm^2. Meanwhile, the predicted September SIE in 2014 is 5.53 Mkm^2 and 0.25 Mkm^2 (or 4.7%) higher than the observed 5.28 Mkm^2. From their forecast error distribution and the forecast value for the latest two years, it suggests that monthly SIE differences in JJ and JA can provide a simple and reliable regression model for forecasting the September SIE over the Arctic.

4. Summary and Conclusion

The association between these monthly SIE differences and atmospheric circulation patterns at SLP, 700 hPa, and 500 hPa GHT and the SST were all examined. As a consequence, major findings and conclusions from this study are as follows.

(1) The monthly SIE difference for June minus July (JJ) has the most growth in past three decades during warm seasons, and this growth has become more evident in the last decade. As an important contribution to the September SIE, it can be used to predict the September SIE decline since it has the most significant correlation. On the other hand, the SIE difference for April minus May (AM) is noted that there is a weakly decreasing trend in the period 1979–2009. The growth rate of JA SIE is lower than the JJ SIE but its average value for 1979–2012 is higher than JJ SIE and its interannual variability has an important contribution in the decline of September SIE. The monthly differences JJ and JA are closely related to the September SIE, and the superposition of the higher JJ and JA SIE results in a stronger decline of SIE in September in 2007 and 2012.

(2) The interannual variability of the JJ SIE is closely related to atmospheric circulation anomaly patterns, and it has significant positive correlation with simultaneous SLP, 700 hPa, and 500 hPa heights in July over the polar regions and high latitudes over eastern Atlantic and with the SST in spring at midlatitudes over central North Pacific and eastern Atlantic. Based on the lag-circulation pattern anomalies, we can use the relation of summer 500 hPa height fields and the SST in spring to understand the JJ SIE variability in close connection to summer atmosphere circulation anomalies and the recent decline of the September SIE.

(3) A combination of preceding SIE differences was explored to further improve predictive ability for the September SIE decline. A simple regression forecasting model for September SIE was established using monthly SIE differences for the JJ and JA, and this provides a statistical tool to predict the September SIE, as well as a useful reference for sea ice dynamical models.

Furthermore, we discussed a possible physical mechanism for the enhancement of SLP and the 500 hPa heights associated with the JJ SIE variations. For example, positive 500 hPa height anomalies in July at high latitudes, together

with high pressure systems and more solar radiation, are favourable for accelerated sea ice melting and consequently decrease of the JJ SIE over the Arctic. While the more localized monthly anomalies such as the SIE in July minus August (JA), which is an important factor to predict the SIE in September, may be attributed to sea ice anomalies themselves or other nonlinear factors such as surface wind turbulence exchange and ocean heat exchange flux besides partly effects of large-scale monthly mean atmosphere circulation, surface wind field with longer time scales such as intraseasonal scales is a better indicator for Arctic sea ice variability in September [33]; however, while comparing SLP and 500 hPa height field, it is found that the surface wind field with monthly scale has a weak correlation relationship with the monthly-to-monthly total sea ice differences in this study (not shown). This needs to be verified by analyzing the connections between the monthly SIE differences and surface wind anomalies with multiscales by further studies in future.

Conflict of Interests

The authors declare that there is no conflict of interests regarding the publication of this paper.

Acknowledgments

This study was supported by science funding from University of Regina. Sea ice extent dataset over the Arctic was provided by the National Snow & ICE Data Center (NSIDC) (http://nsidc.org/data/docs/noaa/g02135_seaice_index/), and NCEP data were provided by the Physical Sciences Division, Earth System Research Laboratory, NOAA, Boulder, Colorado (http://www.esrl.noaa.gov/psd/).

References

[1] G. A. Meehl, T. F. Stocker, W. D. Collins et al., "Global climate projections," in *Climate Change 2007: The Physical Science Basis. Contribution of Working Group I to the Fourth Assessment Report of the Intergovernmental Panel on Climate Change (IPCC)*, S. Solomon, D. Qin, M. Manning et al., Eds., pp. 747–845, Cambridge University Press, Cambridge, UK, 2007.

[2] A. R. Mahoney, R. G. Barry, V. Smolyanitsky, and F. Fetterer, "Observed sea ice extent in the Russian Arctic, 1933–2006," *Journal of Geophysical Research*, vol. 113, no. 11, Article ID C11005, 2008.

[3] P. Y. Groisman, T. R. Karl, R. W. Knight, and G. L. Stenchikov, "Changes of snow cover, temperature, and radiative heat balance over the Northern Hemisphere," *Journal of Climate*, vol. 7, no. 11, pp. 1633–1656, 1994.

[4] A. D. Vernekar, J. Zhou, and J. Shukla, "The effect of Eurasian snow cover on the Indian monsoon," *Journal of Climate*, vol. 8, no. 2, pp. 248–266, 1995.

[5] D. W. J. Thompson and J. M. Wallace, "The Arctic oscillation signature in the wintertime geopotential height and temperature fields," *Geophysical Research Letters*, vol. 25, no. 9, pp. 1297–1300, 1998.

[6] I. G. Rigor, J. M. Wallace, and R. L. Colony, "Response of sea ice to the Arctic Oscillation," *Journal of Climate*, vol. 15, no. 18, pp. 2648–2663, 2002.

[7] R. D. Brown, "Northern Hemisphere snow cover variability and change, 1915-97," *Journal of Climate*, vol. 13, no. 13, pp. 2339–2355, 2000.

[8] H. Ye, "Quasi-biennial and quasi-decadal variations in snow accumulation over Northern Eurasia and their connections to the Atlantic and pacific oceans," *Journal of Climate*, vol. 14, no. 24, pp. 4573–4584, 2001.

[9] H. Ye and Z. Bao, "Lagged teleconnections between snow depth in Northern Eurasia, rainfall in Southeast Asia and sea-surface temperatures over the tropical Pacific Ocean," *International Journal of Climatology*, vol. 21, no. 13, pp. 1607–1621, 2001.

[10] M. C. Serreze, M. M. Holland, and J. Stroeve, "Perspectives on the Arctic's shrinking sea-ice cover," *Science*, vol. 315, no. 5818, pp. 1533–1536, 2007.

[11] C. Deser and H. Teng, "Evolution of Arctic sea ice concentration trends and the role of atmospheric circulation forcing, 1979–2007," *Geophysical Research Letters*, vol. 35, no. 2, Article ID L02504, 2008.

[12] D. Budikova, "Role of Arctic sea ice in global atmospheric circulation: a review," *Global and Planetary Change*, vol. 68, no. 3, pp. 149–163, 2009.

[13] M. Honda, J. Inoue, and S. Yamane, "Influence of low Arctic sea-ice minima on anomalously cold Eurasian winters," *Geophysical Research Letters*, vol. 36, no. 8, Article ID L08707, 2009.

[14] V. Petoukhov and V. A. Semenov, "A link between reduced Barents-Kara sea ice and cold winter extremes over northern continents," *Journal of Geophysical Research D: Atmospheres*, vol. 115, no. 21, Article ID D21111, 2010.

[15] Z. Bao, R. Kelly, and R. Wu, "Variability of regional snow cover in spring over western Canada and its relationship to temperature and circulation anomalies," *International Journal of Climatology*, vol. 31, no. 9, pp. 1280–1294, 2011.

[16] J. Liu, J. A. Curry, H. Wang, M. Song, and R. M. Horton, "Impact of declining Arctic sea ice on winter snowfall," *Proceedings of the National Academy of Sciences of the United States of America*, vol. 109, no. 11, pp. 4074–4079, 2012.

[17] J. Wang and M. Ikeda, "Arctic oscillation and Arctic Sea-Ice oscillation," *Geophysical Research Letters*, vol. 27, no. 9, pp. 1287–1290, 2000.

[18] J. A. Maslanik, C. Fowler, J. Stroeve et al., "A younger, thinner Arctic ice cover: increased potential for rapid, extensive sea-ice loss," *Geophysical Research Letters*, vol. 34, no. 24, Article ID L24501, 2007.

[19] J. Stroeve, M. Serreze, S. Drobot et al., "Arctic sea ice extent plummets in 2007," *Eos Transactions AGU*, vol. 89, no. 2, pp. 13–20, 2008.

[20] R. A. Kerr, "Ice-free arctic sea may be years, not decades, away," *Science*, vol. 337, no. 6102, article 1591, 2012.

[21] I. Mahlstein and R. Knutti, "September Arctic sea ice predicted to disappear near 2°C global warming above present," *Journal of Geophysical Research D: Atmospheres*, vol. 117, no. 6, Article ID D06104, 2012.

[22] J. C. Stroeve, V. Kattsov, A. Barrett et al., "Trends in Arctic sea ice extent from CMIP5, CMIP3 and observations," *Geophysical Research Letters*, vol. 39, no. 16, Article ID L16502, 2012.

[23] C. Deser, J. E. Walsh, and M. S. Timlin, "Arctic sea ice variability in the context of recent atmospheric circulation trends," *Journal of Climate*, vol. 13, no. 3, pp. 617–633, 2000.

[24] M. C. Serreze, J. A. Maslanik, T. A. Scambos et al., "A record minimum arctic sea ice extent and area in 2002," *Geophysical Research Letters*, vol. 30, no. 3, 2003.

[25] M. C. Serreze, A. P. Barrett, and J. J. Cassano, "Circulation and surface controls on the lower tropospheric air temperature field of the Arctic," *Journal of Geophysical Research D: Atmospheres*, vol. 116, no. 7, Article ID D07104, 2011.

[26] J. A. Francis and E. Hunter, "New insight into the disappearing Arctic sea ice," *Eos, Transactions American Geophysical Union*, vol. 87, no. 46, pp. 509–511, 2006.

[27] S. V. Nghiem, I. G. Rigor, D. K. Perovich, P. Clemente-Colón, J. W. Weatherly, and G. Neumann, "Rapid reduction of Arctic perennial sea ice," *Geophysical Research Letters*, vol. 34, no. 19, Article ID L19504, 2007.

[28] M. Ogi and J. M. Wallace, "Summer minimum Arctic sea ice extent and the associated summer atmospheric circulation," *Geophysical Research Letters*, vol. 34, no. 12, Article ID L12705, 2007.

[29] J. Zhang, M. Steele, R. Lindsay, A. Schweiger, and J. Morison, "Ensemble 1-Year predictions of Arctic sea ice for the spring and summer of 2008," *Geophysical Research Letters*, vol. 35, no. 8, Article ID L08502, 2008.

[30] I. G. Rigor and J. M. Wallace, "Variations in the age of Arctic sea-ice and summer sea-ice extent," *Geophysical Research Letters*, vol. 31, no. 9, Article ID L09401, 2004.

[31] J. A. Maslanik, M. C. Serreze, and R. G. Barry, "Recent decreases in Arctic summer ice cover and linkages to atmospheric circulation anomalies," *Geophysical Research Letters*, vol. 23, no. 13, pp. 1677–1680, 1996.

[32] J. C. Rogers, L. Yang, and L. Li, "The role of Fram Strait winter cyclones on sea ice flux and on Spitsbergen air temperatures," *Geophysical Research Letters*, vol. 32, no. 6, Article ID L06709, 2005.

[33] M. Ogi, K. Yamazaki, and J. M. Wallace, "Influence of winter and summer surface wind anomalies on summer Arctic sea ice extent," *Geophysical Research Letters*, vol. 37, no. 7, Article ID L07701, 2010.

[34] M. Ogi and K. Yamazaki, "Trends in the summer northern annular mode and Arctic sea ice," *Scientific Online Letters on the Atmosphere*, vol. 6, pp. 41–44, 2010.

[35] S. D. Drobot, J. A. Maslanik, and C. Fowler, "A long-range forecast of Arctic summer sea-ice minimum extent," *Geophysical Research Letters*, vol. 33, no. 10, Article ID L10501, 2006.

[36] R. W. Lindsay, J. Zhang, A. J. Schweiger, and M. A. Steele, "Seasonal predictions of ice extent in the Arctic Ocean," *Journal of Geophysical Research C: Oceans*, vol. 113, no. 2, Article ID C02023, 2008.

[37] E. Blanchard-Wrigglesworth, K. C. Armour, C. M. Bitz, and E. DeWeaver, "Persistence and inherent predictability of arctic sea ice in a GCM ensemble and observations," *Journal of Climate*, vol. 24, no. 1, pp. 231–250, 2011.

[38] J. W. Hurrell, "Decadal trends in the North Atlantic Oscillation: regional temperatures and precipitation," *Science*, vol. 269, no. 5224, pp. 676–679, 1995.

[39] D. W. J. Thompson and J. M. Wallace, "Annular modes in the extratropical circulation. Part I: month-to-month variability," *Journal of Climate*, vol. 13, no. 5, pp. 1000–1016, 2000.

[40] E. Kalnay, M. Kanamitsu, R. Kistler et al., "The NCEP/NCAR 40-year reanalysis project," *Bulletin of the American Meteorological Society*, vol. 77, no. 3, pp. 437–471, 1996.

[41] S. Zhou, A. J. Miller, J. Wang, and J. K. Angell, "Trends of NAO and AO and their associations with stratospheric processes," *Geophysical Research Letters*, vol. 28, no. 21, pp. 4107–4110, 2001.

[42] R. E. Moritz, C. M. Bitz, and E. J. Steig, "Dynamics of recent climate change in the Arctic," *Science*, vol. 297, no. 5586, pp. 1497–1502, 2002.

[43] M. H. Kutner, C. J. Nachtsheim, and J. Neter, *Applied Linear Regression Models*, McGraw-Hill/Irwin, Boston, Mass, USA, 4th edition, 2004.

[44] C. M. Bitz, M. M. Holland, E. C. Hunke, and R. E. Moritz, "Maintenance of the sea-ice edge," *Journal of Climate*, vol. 18, no. 15, pp. 2903–2921, 2005.

[45] D. R. Cayan, "Latent and sensible heat flux anomalies over the northern oceans: the connection to monthly atmospheric circulation," *Journal of Climate*, vol. 5, pp. 354–369, 1992.

[46] C. Deser and M. S. Timlin, "Atmosphere-ocean interaction on weekly timescales in the North Atlantic and Pacific," *Journal of Climate*, vol. 10, no. 3, pp. 393–408, 1997.

[47] M. Watanabe and M. Kimoto, "On the persistence of decadal SST anomalies in the North Atlantic," *Journal of Climate*, vol. 13, no. 16, pp. 3017–3028, 2000.

[48] A. Czaja and C. Frankignoul, "Influence of the North Atlantic SST on the atmospheric circulation," *Geophysical Research Letters*, vol. 26, no. 19, pp. 2969–2972, 1999.

[49] A. Czaja and C. Frankignoul, "Observed impact of Atlantic SST anomalies on the North Atlantic oscillation," *Journal of Climate*, vol. 15, no. 6, pp. 606–623, 2002.

[50] Q. Liu, N. Wen, and Z. Liu, "An observational study of the impact of the North Pacific SST on the atmosphere," *Geophysical Research Letters*, vol. 33, Article ID L18611, 2006.

[51] J. A. Francis, W. Chan, D. J. Leathers, J. R. Miller, and D. E. Veron, "Winter Northern Hemisphere weather patterns remember summer Arctic sea-ice extent," *Geophysical Research Letters*, vol. 36, no. 7, Article ID L07503, 2009.